NASA TECHNICAL NOTE

NASA TN D-6276

CYCLIC OXIDATION RESISTANCE OF CLAD IN-100 AT 1040° AND 1090° C: TIME, CYCLE FREQUENCY, AND CLAD THICKNESS EFFECTS

by Michael A. Gedwill

Lewis Research Center
Cleveland, Ohio 44135

NATIONAL AERONAUTICS AND SPACE ADMINISTRATION • WASHINGTON, D. C. • JUNE 1971

1. Report No.	2. Government Accession No.	3. Recipient's Catalog No.
NASA TN D-6276		

4. Title and Subtitle	5. Report Date
CYCLIC OXIDATION RESISTANCE OF CLAD IN-100 AT 1040° AND 1090° C: TIME, CYCLE FREQUENCY, AND CLAD THICKNESS EFFECTS	June 1971
	6. Performing Organization Code
7. Author(s)	8. Performing Organization Report No.
Michael A. Gedwill	E-6108
	10. Work Unit No.
9. Performing Organization Name and Address	129-03
Lewis Research Center National Aeronautics and Space Administration Cleveland, Ohio 44135	11. Contract or Grant No.
	13. Type of Report and Period Covered
12. Sponsoring Agency Name and Address	Technical Note
National Aeronautics and Space Administration Washington, D.C. 20546	14. Sponsoring Agency Code

15. Supplementary Notes

16. Abstract

Furnace oxidation studies were conducted on nickel alloy IN-100 specimens clad with Ni-20Cr-4Al-1.2Si, Fe-25Cr-4Al-1Y, and Ni-30Cr-1.4Si foils (0.051 to 0.254 mm thick). The Ni-Cr-Al-Si cladding was the most protective on IN-100 at both temperatures and was rather insensitive to cladding thickness in the range studied, to cycle frequency, and to exposure time up to 400 hours. The protection offered by the Ni-Cr-Al-Si cladding was comparable to that provided by a commercial aluminide coating. The Fe-Cr-Al-Y cladding was moderately protective and the Ni-Cr-Si was least protective. The performance of all three cladding systems was affected by interdiffusion with IN-100.

17. Key Words (Suggested by Author(s))
Claddings
Superalloy Protection
Oxidation Resistance

18. Distribution Statement
Unclassified - unlimited

19. Security Classif. (of this report)	20. Security Classif. (of this page)	21. No. of Pages	22. Price*
Unclassified	Unclassified	43	$3.00

*For sale by the National Technical Information Service, Springfield, Virginia 22151

CYCLIC OXIDATION RESISTANCE OF CLAD IN-100 AT 1040° AND 1090° C: TIME, CYCLE FREQUENCY, AND CLAD THICKNESS EFFECTS

by Michael A. Gedwill

Lewis Research Center

SUMMARY

Cyclic furnace testing was used to examine the effects of cladding thickness, exposure time, cycle frequency, and temperature on the oxidation behavior of three clad IN-100 systems. The three claddings, Ni-20Cr-4Al-1.2Si, Fe-25Cr-4Al-1Y, and Ni-30Cr-1.4Si as foils ranging from 0.051 to 0.254 millimeter in thickness, were diffusion bonded to IN-100 and oxidation tested. Total exposure times up to 400 hours using 1- and 20-hour cycles were employed. Test temperatures were 1040° and 1090° C. Similar tests were conducted on the cladding themselves, on commercial aluminide-coated IN-100, and on unprotected IN-100. Evaluations were based primarily on gravimetric, metallographic, and surface recession analyses.

At both temperatures, Ni-20Cr-4Al-1.2Si was the most protective cladding on IN-100; the least protective cladding was Ni-30Cr-1.4Si. The oxidation behavior of the former cladding in the thicknesses evaluated was rather insensitive to cycle frequency, to cladding thickness, or to test time up to 400 hours. Its protection was comparable to that provided by a widely used commercial aluminide coating. The lives of the other two claddings on IN-100 were extended by increases in the cladding thickness. The 0.127-millimeter Ni-20Cr-4Al-1.2Si and Fe-25Cr-4Al-1Y claddings fully protected IN-100 for up to 400 hours at 1040° C, but only the former appeared capable of much longer exposures. Under these test conditions, even a thinner (0.051 mm) Ni-20Cr-4Al-1.2Si cladding could adequately protect IN-100 for 400 hours at both temperatures.

The experimental data indicated that the oxidation resistance of the three clad systems was degraded to various degrees by interdiffusion. Up to at least 200 hours oxidation at 1040° C, however, this effect was small for the 0.127-millimeter-thick Ni-20Cr-4Al-1.2Si cladding on IN-100.

INTRODUCTION

The efficiency and performance of aircraft gas turbine engines are significantly improved as the turbine operating temperatures are increased. Higher temperatures, however, produce increased oxidation of the turbine components. For this reason, protective coatings are continuously being developed for nickel- and cobalt-based superalloys (ref. 1). In a previous study (ref. 2) the feasibility of protecting the nickel superalloy IN-100 and the cobalt superalloy WI-52 with low-strength, highly oxidation-resistant metallic claddings (0.127 mm thick) of Ni-30Cr-1.4Si; Ni-20Cr-4Al-1.2Si; and Fe-25Cr-4Al-1Y was explored. Furnace oxidation tests on diffusion-bonded, completely encapsulated specimens were conducted at 1040° and 1090° C for up to 200 hours using 20-hour cycles. For IN-100, all three claddings were effective in providing 200 hours of protection at 1040° C. At 1090° C, only the Ni-20Cr-4Al-1.2Si cladding afforded good protection for 200 hours.

The present study was conducted to further examine the oxidation behavior and protection potential of these claddings on IN-100 for longer exposure times and with more frequent thermal cycling in order to more closely approximate anticipated service conditions. Also, it was necessary to see if thinner claddings would perform as well as those previously studied or if much thicker claddings are needed to extend the life of the systems. Cladding thicknesses examined were 0.051, 0.127, and 0.254 millimeter (0.002, 0.005, and 0.010 in.). Cycle frequencies of 1 hour and 20 hours were used and furnace oxidation tests were extended to 400 hours at both 1040° and 1090° C. The evaluation of protection was based primarily on gravimetric analysis, metallographic examination, and cladding surface recession. Supplemental analyses included X-ray diffraction (XRD), X-ray fluorescence (XRF), electron microprobe (EMP), and tensile testing. In addition, the cyclic oxidation behavior of these systems was compared to that obtained for the cladding alloys bonded to themselves, to IN-100 protected by a widely used proprietary commercial aluminide coating, and to unprotected IN-100.

EXPERIMENTAL PROCEDURES

Materials and Specimen Preparation

Table I gives the chemical analysis of the cast IN-100 and the Ni-30Cr-1.4Si (Ni-Cr-Si), the Ni-20Cr-4Al-1.2Si (Ni-Cr-Al-Si), and the Fe-25Cr-4Al-1Y (Fe-Cr-Al-Y) foils. The IN-100 was cast to 50.8-millimeter by 25.4-millimeter by 2.5-millimeter coupons. The Ni-Cr-Si and Ni-Cr-Al-Si foils were obtained in 0.051-, 0.127-, and 0.254-millimeter thicknesses and as 2.54-millimeter plate. The Fe-Cr-Al-Y was only available in the latter two foil thicknesses and in the same thickness plate.

Face sheets and picture frames of the cladding materials were surface prepared and gas-pressure diffusion bonded to IN-100 coupons and also to cladding plate specimens in canned assemblies using the procedures of reference 2 (2 hr at 1090° C and 103-MN/m^2 (15 000-psi) helium pressure). Before bonding, the cladding components were degreased, chemically cleaned, and subsequently cleaned in acetone and then in alcohol. The IN-100 substrates were vapor blasted, followed by cleaning in acetone and then in alcohol.

Several as-cast IN-100 specimens were also coated with a widely used, proprietary commercial aluminide coating. This coating was deposited to a thickness of about 0.043 millimeter on IN-100.

Cyclic Oxidation Testing

Specimens were cyclic oxidation tested at 1040° and 1090° C for up to 400 hours in furnaces controlled to ±5° C. Some specimens were placed in alumina boats and manually cycled in and out of a horizontal, multitube furnace at 20-hour intervals (as described in ref. 2). During testing, filtered air (0.05 m^3/hr) was passed through the alumina tubes. After each exposure the specimens were cooled to room temperature, lightly brushed, and weighed. Other specimens were individually suspended from platinum wires and automatically raised and lowered into a vertical, multitube furnace at 1-hour intervals. After each exposure, the specimens were cooled to approximately 100° C in 10 minutes before being reinserted. Here natural convection maintained the airflow through the furnace. At various times the specimens were cooled to room temperature, lightly brushed, and weighed. Although not determined, it is believed that the oxidizing environment in the horizontal and vertical furnaces was similar.

Additional Evaluations

Cross sections of specimens were metallographically examined to determine the structural changes (and degradation) that occurred during cladding and oxidation. These examinations were made at magnifications up to ×750 using bright-field and polarized-light illumination. Surface recession - oxide penetration data were calculated from measurements obtained from photomicrographs. Figure 1 illustrates the method used in calculating the surface recession data. A hand micrometer was used to measure the nominal thicknesses of the cladding foils before bonding. Since thickness measurement of the cladding in each specimen was not made prior to either bonding or testing, the recession data must only be viewed as approximations.

X-ray diffraction (XRD) and X-ray fluorescence (XRF) analyses were performed on oxidizer specimens to determine the structures and approximate compositions of the retained surface scales. XRD was made either on as-scraped or on in-situ scales, whereas XRF was always made on the in-situ scales. The spall products were analyzed only by XRD. Summaries of the XRD and XRF analyses are given in appendix A.

Selected specimens were also examined in an electron microprobe (EMP) to determine the extent of interdiffusion, concentration variations, and segregation of major and minor elements. Two EMP techniques were used. One technique, the most widely used, consisted of obtaining X-ray raster micrographs for major and selected minor elements in the oxide scales and the clad portions. The raster micrographs, taken at a magnification of ×500, showed qualitatively the distribution of the elements but provided no quantitative information. In the other technique, uncorrected concentration line scans across the specimens were obtained, in general, only for the major elements. Summaries of all the EMP data are contained in appendix B.

Limited tensile tests were conducted on the most oxidation resistant system (Ni-Cr-Al-Si clad IN-100) to determine the combined effects of oxidation and interdiffusion on tensile properties. A completely clad IN-100 specimen was subjected to cyclic oxidation at 1040° C. After oxidation, the specimen was machined into two tensile specimens of the design shown in figure 2. An as-clad IN-100 specimen was similarily machined into tensile specimens. The two tensile specimens were tested at a crosshead speed of 1.27 millimeters per minute at 1040° C in argon. For strength calculations, the approximate cross-sectional area of the IN-100 substrate before bonding was used.

RESULTS AND DISCUSSION

The most oxidation-resistant system was Ni-Cr-Al-Si clad IN-100 followed by the less resistant Fe-Cr-Al-Y clad IN-100 and the very poorly resistant Ni-Cr-Si clad IN-100. The results and discussion that follow are presented in the order of decreasing oxidation resistance.

Ni-Cr-Al-Si Clad IN-100

Weight change and metallography. - The effects of cladding thickness and cycle frequency on the weight changes of Ni-Cr-Al-Si clad IN-100 up to 400 hours of oxidation exposure are presented in figure 3. For all the test conditions studied, the clad test specimens initially gained weight for some period, after which a gradual weight loss occurred. Figure 3(a) contains data from 1040° C exposures using both 1- and 20-hour cycles. This figure shows that for 1-hour cycles both the times to initial net weight

loss and the extent of weight loss are related to cladding thickness. The thicker the clad, the more protective it is. Also decreasing the cycle frequency from 1-hour cycles to 20-hour cycles is about as beneficial as increasing cladding thickness from 0.127 to 0.254 millimeter. Although at 1040° C the weight change behavior appears to be influenced by the cladding thickness and cycle frequency, subsequent metallographic examination showed that in reality this system was rather insensitive to these two variables. At 1090° C, using 20-hour cycles, weight loss after a 200-hour exposure appeared directly related to cladding thickness (fig. 3(b)). However, the differences between specimens of different cladding thicknesses were very small. Metallographic examination showed that the thinner clads had suffered greater grain boundary oxidation. The oxide scales, composed principally of $NiCr_2O_4$, NiO, and SiO_2 (appendix A), were anchored more firmly on the specimens with the thinnest clads and less of the scales which formed spalled off. At both temperatures, the oxidation resistance of the clad specimens, as judged by weight change behavior, was significantly better than that for the unprotected IN-100.

Figure 4 contains cross-sectional photomicrographs of the 0.051-, 0.127-, and 0.254-millimeter claddings on IN-100 after 400 1-hour cycles at 1040° C. In all cases the claddings protected IN-100 for the full 400-hour test time. Regardless of cladding thickness, little grain boundary or twin boundary oxidation was observed in this system. Also, there was little difference in the thickness of the visibly affected diffusion zone in the IN-100 beneath the various thicknesses of cladding. Extensive amounts of a round, cream-colored phase developed in the clad just above the bond interface during oxidation in the 0.051-millimeter-clad specimen and this phase was observed to exist in lesser amounts in the thicker claddings.

In figure 5, microstructures after various 20-hour cycles at both 1040° and 1090° C can be examined. During the early stages of oxidation (fig. 5(a)) some intragranular oxidation occurred. Thereafter the attack occurred along a planar front. The gradual consumption of cladding with exposure time can be seen by comparing figures 5(a-1), (a-2), and (a-3) or figures 5(b-1) and (b-2). Upon comparison of figures 4(b) and 5(a-3), it can be seen that different cycle frequency produced little difference in the extent of oxidation in the 400-hour - 1-hour-cycled specimen and the 400-hour - 20-hour-cycled specimen. A comparison of figures 5(a-2) and (b-2) - both ten 20-hour cycles at 1040° and 1090° C, respectively - shows greater oxidation attack at 1090° C, as evidenced by less remaining cladding. While time at 1040° C had a small effect on the growth of the visibly affected diffusion zone in the IN-100 (figs. 5(a-1) to (a-3)), the zone grew more rapidly at 1090° C. Also higher temperature exposure appeared to result in more oxide spalling (compare figs. 5(a-2) and (b-2)). This observation was supported by the weight loss data at 1090° C presented in figure 3(b).

Thus, the influence of cycle frequency and exposure time up to 400 hours appears minor, while exposure temperature appears to be the major factor controlling the life of Ni-Cr-Al-Si claddings on IN-100.

Surface recession. - Using the criteria presented in figure 1, residual cladding thickness was measured metallographically. The data are presented in table II (Ni-Cr-Al-Si cladding on Ni-Cr-Al-Si plate) and table III (Ni-Cr-Al-Si on IN-100). These data are summarized in figure 6 as calculated, total, cladding surface recession data.

Figure 6(a) shows that, for both 1090° C - 20-hour cycles and 1040° C - 1-hour cycles, increasing cladding thickness appears to result in higher total surface recession but also in higher percentages of residual useful cladding after test. The data for the two test conditions are within a fairly large scatterband. For each test condition the differences in total surface recession are generally minor, indicating again that under these conditions cladding thickness exerted a minor (if any) influence on surface recession. Figure 6(b) shows that after an initial small amount of surface recession the effect of an increased number of 20-hour cycles (up to maximum of 20 cycles) on surface recession is minor. Figure 6(c) shows that the 0.051- and 0.127-millimeter clads on IN-100 (as well as clad Ni-Cr-Al-Si) exhibited increased surface recession with temperature, as expected. Here it appears that in ten 20-hour cycles the Ni-Cr-Al-Si clad IN-100 was somewhat less prone to surface recession regardless of thickness than was Ni-Cr-Al-Si clad Ni-Cr-Al-Si. The reason for this difference is not clear. It is felt, however, that the recession data in conjunction with the metallographic observations indicate that the thinner 0.051-millimeter Ni-Cr-Al-Si cladding protected IN-100 as well as the thicker 0.127-millimeter cladding at both temperatures. Also, no significant benefit in extending the lifetime of the Ni-Cr-Al-Si clad IN-100 system is realized by further increasing the cladding thickness to 0.254 millimeter.

Tensile testing. - Since the Ni-Cr-Al-Si clad IN-100 system showed promising oxidation resistance for 400 hours at 1040° C, tensile tests were conducted on it to determine the effects of oxidation and interdiffusion on mechanical properties. Duplicate tensile specimens, as clad and as oxidized for 400 hours at 1040° C using 1-hour cycles, were machined as shown in figure 2. For comparison purposes, a bare (unprotected) IN-100 specimen was given a duplex thermal treatment in argon to simulate the bonding and exposure cycle times and then was also machined into duplicate tensile specimens. The results of tensile tests on these specimens at 1040° C are presented in figure 7.

During oxidation of the Ni-Cr-Al-Si clad IN-100 system, the strengths decreased while the elongation increased. The 1040° C strengths of the system were about 28 percent lower after 400 hours oxidation at 1040° C than as clad. This system also showed decreases in strengths of about 40 percent after oxidation when compared to data for thermally treated, bare IN-100. Assuming a reaction zone thickness of 0.098 millimeter on both sides of the IN-100 substrates (based on electron microprobe analysis, appendix B) and decreasing the substrate areas by a corresponding amount in the strength calculations, the interdiffusion effect could account for only about 12 percent of the losses. Further clarification by more extensive testing is required.

Fe-Cr-Al-Y Clad IN-100

In comparison to Ni-Cr-Al-Si, the Fe-Cr-Al-Y clads on IN-100 were slightly less protective at 1040° C and much less protective at 1090° C.

Weight change and metallography. - The effects of cladding thickness and cycle frequency on the weight change of Fe-Cr-Al-Y clad IN-100, Fe-Cr-Al-Y clad Fe-Cr-Al-Y, and bare IN-100 up to 400 hours of oxidation exposure are presented in figure 8. Figure 8(a) contains data from 1040° C exposures. One of the 0.127-millimeter-clad specimens was exposed at 1-hour cycles; all the others and the bare IN-100 were given 20-hour cycles. Here none of the oxide scales on the 20-hour-cycled clad specimens spalled significantly, but the oxides on bare IN-100 continued to spall on each cycle. The 1-hour-cycled specimen (0.127-mm clad) began spalling after about 240 hours. This situation led to the eventual downturn in its weight change curve. Under the same conditions, the 0.254-millimeter-clad IN-100 showed lower weight gains than the 0.127-millimeter-clad IN-100, but similar to those of the Fe-Cr-Al-Y clad Fe-Cr-Al-Y. This suggests that interdiffusion between clad and substrate elements caused a degrading effect on the oxidation resistance of the 0.127-millimeter cladding. This was not realized in the weight change behavior of the thicker (0.254 mm) cladding within the test time employed. At 1090° C (fig. 8(b)) this same relation between weight change was observed for the two clads on IN-100. After 200 hours the weight gains of the clad specimens were from 1 to 2 milligrams per square centimeter greater at this temperature than at 1040° C. Spalling from the bare IN-100 was heavy; from the 0.127-millimeter-clad IN-100 it was light medium; from the 0.254-millimeter-clad IN-100 it was very light.

The effects of time, cycle frequency, and exposure temperature on the microstructures of as-oxidized specimens of Fe-Cr-Al-Y clad IN-100 are shown in figure 9. Here increasing exposure time, cycles, and temperature produced increases in the amount of internal and grain boundary oxidation. Beneath the cladding, extensive interdiffusion zones were observed in all cases. Figure 9(c) shows this diffusion zone to be thinner with increased cycle frequency as compared to that shown in figure 9(b). This is probably due to enhanced outward diffusion of primarily Al to reform the spalling oxide scale, which consisted mainly of αAl_2O_3 and $(Cr, Fe)_2O_3$ (appendix A). Higher temperature exposure at 1090° C (fig. 9(d)) expanded the zone greatly and also seemed to cause the phases that developed in this zone at both temperatures to undergo some resolutioning.

At 1090° C, the Fe-Cr-Al-Y clad IN-100 specimens developed very large surface oxide nodules, as shown in figure 10(a). These nodules penetrated into the diffusion zone beneath the cladding and are believed to be extensions of some of the more severe intergranular oxidation observed in figure 9(d). Generally, polarized light examination of the oxidized clad IN-100 specimens indicated large charcoal black and brown areas

(probably a spinel), white areas (αAl_2O_3), and green areas (Cr_2O_3). Subsequent EMP analyses (appendix B) showed these nodules to be very rich in Al. Similar nodules have been reported on oxidized Fe-Cr, Fe-Cr-Al, and Fe-Ni alloys (ref. 3).

Surface recession. - The cladding surface recession data (measured as shown in fig. 1) are presented in tables II and III. The data are summarized in figure 11. This figure shows that surface recession was greatly reduced (about 50 percent) at both temperatures by increasing the thickness of the cladding from 0.127 to 0.254 millimeter (fig. 11(a)). At 1040° C, the 0.127-millimeter cladding showed only a slight change in surface recession between 200 and 400 hours after an initial, but appreciable, increase (fig. 11(b)). Also as expected, the lower the temperature, the less the surface recession for both thicknesses of Fe-Cr-Al-Y cladding on IN-100 (fig. 11(c)). At both temperatures, however, the thicker cladding on IN-100 experienced slightly greater surface recession than the cladding alloy specimen, but much less than the thinner cladding.

It is believed that these data coupled with the weight change and metallographic results indicate that clad-substrate interdiffusion had a highly significant influence on the oxidation behavior of this system. Furthermore, these results suggest that thicker (greater than 0.127 mm) Fe-Cr-Al-Y claddings are required to extend the life of this system at 1040° C and above.

Ni-Cr-Si Clad IN-100

Of the three systems investigated, the Ni-Cr-Si clad IN-100 system showed the least oxidation resistance at the two test temperatures.

Weight change and metallography. - The protective ability of Ni-Cr-Si claddings on IN-100 was relatively poor, as shown in figure 12. At 1040° C, only the 0.254-millimeter cladding approached the behavior of Ni-Cr-Si clad Ni-Cr-Si. The thinner claddings gained weight rapidly and while the 0.051-millimeter clad specimen showed large weight gains at 60 and 180 hours, the 0.127-millimeter cladding gained almost 6 milligrams per square centimeter and then lost weight rapidly. Spalling began early for the 0.051-millimeter cladding and after 120 hours for the 0.127-millimeter-clad IN-100. At 1090° C both cladding thicknesses showed sporadic weight gains, followed by significant losses.

The poor oxidation resistance of the Ni-Cr-Si clad IN-100 can also be observed in figure 13, which contains cross-sectional photomicrographs of the various thickness claddings after several exposure times at both 1040° and 1090° C. All specimens were given 20-hour cycles. After 200 hours of exposure at 1040° C, figures 13(a) to (c) show that the 0.051-millimeter clad was completely penetrated by oxides; oxides penetrated about one-half of the 0.127-millimeter clad; and only the heaviest cladding, 0.254 millimeter, was relatively unharmed. X-ray diffraction analyses indicated that the oxides

were primarily $NiCr_2O_4$ and Cr_2O_3 (appendix A). After 400 hours (fig. 13(d)), however, the 0.127-millimeter clad was almost completely penetrated by oxides at 1040° C. At 1090° C, the depth of attack increased and considerably more intergranular oxides were present (figs. 13(e) and (f)). The 0.254-millimeter cladding was still somewhat protective after 200 hours.

Since the oxidation resistance of the Ni-Cr-Si and Ni-Cr-Al-Si claddings on themselves are very similar (ref. 2), it might have been expected that these two claddings on IN-100 would behave in a similar manner during oxidation. The results reported herein show that this was not the case. It is felt that clad-substrate interdiffusion had a significant, but detrimental, influence on maintaining the protective scale formed on the Ni-Cr-Si claddings, whereas the scale formed on the Ni-Cr-Al-Si claddings was relatively unaffected by interdiffusion.

Surface recession. - Surface recession data are presented in table III and summarized in figure 14. Figure 14(a) shows that either the thicker the cladding or the lower the temperature, the less total surface recession after ten 20-hour cycles. The surface recession of the 0.254-millimeter cladding was about one-tenth that of the 0.127-millimeter cladding after 200 hours exposure at 1040° C. Also after 200 hours exposure, surface recession for the 0.254-millimeter-clad specimens was greater by a factor of 6 at 1090° C than at 1040° C. Figure 14(b) shows that increased exposure time produced greater surface recessions. The 1040° C data show a less rapid increase with time than the 1090° C data.

These weight change, metallographic, and recession data indicate that Ni-Cr-Si claddings thicker than 0.127 millimeter are required to protect IN-100 from oxidation at the temperatures and times investigated in this study.

Comparison of Clad IN-100 Systems

Figure 15 presents a comparison of the microstructures (figs. 5(c), 9(b), and 13(d)) of the three 0.127-millimeter claddings on IN-100 after 400 hours cyclic oxidation at 1040° C. The three specimens were tested using 20-hour cycles. These photomicrographs clearly show that the Ni-Cr-Al-Si cladding was the most protective, while Ni-Cr-Si was the least protective cladding. The Ni-Cr-Al-Si cladding (fig. 15(a)) shows very little oxidation attack, a uniform protective oxide scale, and essentially no grain boundary oxidation. The Fe-Cr-Al-Y cladding (fig. 15(b)) shows internal and grain boundary oxidation which is much less extensive than that developed in the Ni-Cr-Si cladding (fig. 15(c)). It is apparent that both the Ni-Cr-Al-Si and Fe-Cr-Al-Y claddings fully protected IN-100 for up to 400 hours at 1040° C. However, only the Ni-Cr-Al-Si cladding on IN-100 appears to be capable of surviving much longer exposures. The protective ability of Ni-Cr-Si cladding on IN-100 is limited since the 0.127-millimeter

cladding was almost completely penetrated by oxides within the 400 hours of oxidation at 1040° C.

In all three systems, the protective oxide scales on the claddings were apparently affected to varying degrees by interdiffusion between the cladding and substrate elements. X-ray fluorescence analyses (appendix A) indicated that Mo, Ti, and Co diffused readily into all three claddings from IN-100. The three photomicrographs of figure 15 show diffusion-affected zones beneath the claddings in the IN-100 substrate. The zone was the thickest in the Fe-Cr-Al-Y clad system and the thinnest in the Ni-Cr-Al-Si clad system. Electron microprobe analyses (appendix B) showed that after 200 hours exposure at 1040° C, only the 0.127-millimeter Ni-Cr-Al-Si cladding was not completely penetrated by Ti and Co, but at 1040° C all three 0.127-millimeter claddings were completely penetrated by Ti, Co, and Mo. It is felt that the protective lifetimes and temperature capabilities of these systems could be extended if suitable diffusion barriers were incorporated between the claddings and the IN-100. Under the test conditions employed, generally the three claddings on themselves exhibited similar oxidation resistance (ref. 2) but behaved differently on IN-100. It is believed that these differences can be ascribed to varying degrees of clad-substrate interdiffusion and subsequent interactions with the protective scales. More detailed studies of each system, however, would be required to resolve these differences.

Comparison of Ni-Cr-Al-Si Clad IN-100 With Aluminide-Coated IN-100

The weight change behavior of a widely used, proprietary commercial aluminide coating (0.043 mm thick) on IN-100 is compared to the Ni-Cr-Al-Si cladding (0.051 mm thick) on IN-100 in figure 16. Data in this figure cover up to ten 20-hour cycles at both 1040° and 1090° C. At both temperatures, the aluminide coating gradually gained weight. While no spalling was observed at 1040° C, very light spalling was detected at 1090° C. The cladding gained weight more rapidly at both temperatures, but also showed weight losses which were related to test temperature and which were due to very light to moderate spalling.

Figure 17 offers a pictorial comparison of cross sections of aluminide-coated and Ni-Cr-Al-Si clad IN-100 after testing. The oxide scale on the coating appeared thinner at both temperatures, which makes it less prone to spalling. From a microstructural standpoint, both systems appeared to be about equal in protective ability; and thus, advanced evaluation in simulated engine environments appears warrented. Since the cladding contained only 3.51 percent Al, it may be that by increasing its aluminum content, the cladding would also form a thinner α Al_2O_3 scale and perhaps surpass the protection afforded by the coating. This factor should be examined under static furnace conditions and perhaps under conditions more closely approximating a gas turbine environment.

Although the oxidation resistance of the Ni-Cr-Al-Si cladding on IN-100 was not better than that of the commercial aluminide coating at these temperatures, it is believed that the cladding has an inherent advantage. The cladding may be useful where greater ductility is required (e.g., at the roots of turbine blades). Also, since aluminide coatings on turbine blades are susceptible to fatigue and foreign object damage, a ductile, oxidation-resistant cladding between a brittle aluminide coating and a substrate of low ductility may be highly desirable.

SUMMARY OF RESULTS

A study was conducted to examine the effects of furnace exposure time, clad thickness, cycle frequency, and temperature on the oxidation behavior of clad IN-100. Three claddings were studied: Ni-20Cr-4Al-1.2Si, Ni-30Cr-1.4Si, and Fe-25Cr-4Al-1Y. Each cladding, diffusion bonded to IN-100, was furnace oxidation tested at both 1040° and 1090° C in thicknesses of 0.051 (except Fe-Cr-Al-Y), 0.127, and 0.254 millimeter for times to 400 hours. One-hour and 20-hour cyclic exposures at test temperature were employed. Similar tests were conducted on the claddings bonded to themselves, on commercially aluminide-coated IN-100, and on unprotected IN-100. Evaluations were based primarily on gravimetric, metallographic, and surface recession analyses.

At both temperatures, the Ni-Cr-Al-Si cladding was the most protective on IN-100. Under the test conditions and cladding thicknesses employed it was rather insensitive to cladding thickness, test time up to 400 hours, or to cycle frequency at 1040° C. It was also insensitive to cladding thickness at 1090° C. While Mo, Ti, and Co readily diffused from the IN-100 into all three claddings, these elements appeared not to significantly degrade the protective ability of the Ni-Cr-Al-Si cladding. Both 0.051- and 0.127-millimeter-thick Ni-Cr-Al-Si clads protected IN-100 from oxidation at 1040° and 1090° C for the full 400-hour test time. In the less protective Fe-Cr-Al-Y and the poorly protective Ni-Cr-Si IN-100 systems, system life was extended by increased cladding thickness. At 1040° C, the Fe-Cr-Al-Y cladding on IN-100 was more rapidly degraded by increased cycle frequency than was Ni-Cr-Al-Si. Since both the Fe-Cr-Al-Y and Ni-Cr-Si clad IN-100 systems exhibited rapid and apparently harmful interdiffusion with IN-100, suitable diffusion barriers might extend the lifetimes and use temperature of these clads on IN-100.

The protection of the Ni-Cr-Al-Si cladding was comparable to a widely used commercial aluminide coating. Thus, advanced evaluation in simulated engine environments

appears warrented, since the more ductile cladding alloy may offer advantages such as improved thermal-fatigue resistance.

Lewis Research Center,
National Aeronautics and Space Administration,
Cleveland, Ohio, February 5, 1971,
129-03.

APPENDIX A

X-RAY DIFFRACTION (XRD) AND FLUORESCENCE (XRF) ANALYSES

Table IV contains summaries of XRD and XRF analyses on retained oxide scales and spalls for clad IN-100 systems. Results and discussion pertinent to each system are presented separately, beginning with the most oxidation-resistant system.

Ni-Cr-Al-Si Clad IN-100 System

The XRD data showed that the major constituents of all the retained oxide scales and the spalls from Ni-Cr-Al-Si clad IN-100 specimens were a $NiCr_2O_4$-type spinel and NiO. At 1040° C, αAl_2O_3 and Cr_2O_3 were also frequently observed as minor phases, while at 1090° C a spinel (probably $NiAl_2O_4$) was commonly detected in trace quantities. Although present in large quantities, as indicated in the electron microprobe raster micrographs, Si-containing constituents were not detected by XRD, indicating that this element was probably present as amorphous SiO_2. The XRF data indicated that in varying degrees, more or less dependent on cladding thickness, increased Si, To, Mo, and Co intensities were observed at the cladding surfaces after oxidation for both exposure temperatures. While Si was contained in the cladding, the other elements diffused outward from the IN-100. The XRF data showed that the Al intensity at all thicknesses decreased with time when using 20-hour cycles at 1040° C (except for the three 400-hour - 1-hour-cycled specimens), while it increased at 1090° C.

In general, comparison of elemental distributions with the surface recession data tend to indicate that the presence of Ti and Co in the scale may have been beneficial. For example, the oxidized 0.051-millimeter-clad IN-100 specimens showed Ti and Co in the scales (table IV); from figure 6(a) these show the lowest total recession at both temperatures. The author believes, however, that Al and its concentration in the cladding was more influential in the formation of a protective scale than the other elements in the Ni-Cr-Al-Si clad IN-100 system. The XRF data for the 1040° C oxidized specimens indicated that generally an improvement in the oxidation resistance of a specimen (as reflected in the weight change behavior) corresponded to an increase in Al intensity. For example, figure 3(a) shows that between 300 and 400 hours the 20-hour-cycled, 0.127-millimeter-clad specimen lost weight and Al intensity decreased, while the 1-hour-cycled, 0.127-millimeter-clad specimen's weight change was approaching a constant weight value and this specimen showed a significant increase in Al intensity. All the 1090° C oxidized specimens also showed increases in Al intensity at the surfaces but these specimens were analyzed by XRF when their weight changes were approaching

constant values (see fig. 3(b)). The author believes that the apparent surface enrichment in Al in these latter specimens resulted, in part, from diffusion from the IN-100 substrates.

Most phases must be present in concentrations of from 1 to 5 percent in order to be detected by XRD. Since many oxide constituents can be more readily detected at lower concentrations by polarized-light metallography (ref. 4), the cross sections of oxidized specimens were so examined in this study. All the clad IN-100 and clad cladding-alloy specimens, oxidized at both temperatures, showed the presence of white αAl_2O_3, with the exception of the 0.051-millimeter-clad IN-100 specimens exposed for 10 or more 20-hour cycles at both 1040° and 1090° C. Only six out of 10 oxidized specimens, including three oxidized Ni-Cr-Al-Si clad Ni-Cr-Al-Si specimens analyzed by XRD showed the presence of trace amounts of αAl_2O_3. This finding, along with the XRF and XRD, indicates that during oxidation of the 0.051-millimeter-clad IN-100 specimens aluminum is depleted from the thinnest cladding to the point that αAl_2O_3 can no longer form.

Fe-Cr-Al-Y Clad IN-100 System

The surface oxide scales on the Fe-Cr-Al-Y clad IN-100 specimens were primarily αAl_2O_3 and $(Cr, Fe)_2O_3$, consistent with those observed on the Fe-Cr-Al-Y clad Fe-Cr-Al-Y. The spall collected after 400 1-hour cycles at 1040° C also contained a spinel of the $NiCr_2O_4$ type. For the 1090° C, 200-hour - 20-hour-cycled specimen, XRD failed to detect the spinel nodules which were shown to exist in figure 10 under polarized-light illumination. From all the evidence, the presence of this spinel indicates impending failure of the cladding's protection ability. At both temperatures and for both cladding thicknesses, the XRF data indicated higher concentrations of Ni, Co, Ti, and Mo at the clad IN-100 specimen surfaces after oxidation, reflecting outward diffusion from the IN-100. With the exception of the 0.254-millimeter-clad specimen at 1040° C, Al was observed to decrease at the surface.

Ni-Cr-Si Clad IN-100 System

At both temperatures, the scales on Ni-Cr-Si clad IN-100 specimens were rich in Cr_2O_3 and in $NiCr_2O_4$-type spinels. The failed 0.051-millimeter cladding at 1040° C also showed NiO, $CoCrO_4$, and a low a_o spinel which was probably $NiCo_2O_4$. Polarized-light metallographic examination of these scales and those on oxidized Ni-Cr-Si clad Ni-Cr-Si specimens indicated varying amounts of the dark-brown and black spinel and green Cr_2O_3. However, only Cr_2O_3 was detected by XRD on the

Ni-Cr-Si clad Ni-Cr-Si (ref. 2). The XRF analyses indicated that generally the oxide scales contained increased quantities of Co, Ti, and Mo from IN-100. Since the cladding contained only a trace of Al, its rapid loss by oxide spalling and/or interdiffusional dilution would be expected.

APPENDIX B

ELECTRON MICROPROBE (EMP) ANALYSIS

Table V contains summaries of EMP analyses of raster micrographs and line scans made on selected clad cladding-alloy specimens and on 0.127-millimeter claddings on IN-100. Some of these data are presented in figures 18 to 20. These data are discussed separately, beginning with the most oxidation-resistant system.

Ni-Cr-Al-Si Clad IN-100 System

The schematic raster micrographs in figure 18(a) show that the oxide scales (far left side of clad) on the Ni-Cr-Al-Si clad IN-100 specimens were rich in Ni, Cr, Si, and Mn. In addition, diffusion of Mo, which was very rapid, and that of Co and Ti from IN-100 into the Ni-Cr-Al-Si cladding was directly related to both exposure time and temperature. The concentrations of Ti in the clad near and within the original cladding-substrate interfaces was very high. The high Ti areas near the interfaces coincide with the cream-colored particles, previously observed in figures 4 and 5. Titanium was also highly concentrated in the as-bonded interface. Some sporadic Al-rich regions were also observed at the original interface.

Three sets of line scan EMP data are presented for Co, Cr, and Ni in figure 18(b). These illustrate (1) the effect of exposure time - 200 hours against 400 hours - at 1040° C; (2) the effect of cycle frequency at 1040° C; and (3) the effect of exposure temperature after ten 20-hour cycles. This figure reflects, by the lengths of the bars, the depth of regions whose concentration is different from that of the cladding or the IN-100 for selected elements. The numbers at the ends of the bars give first-approximation weight percentages for these elements. Since these data are in the form of relative X-ray intensity measurements, they are semiquantitative. In regard to exposure time at 1040° C, increasing the time from 200 to 400 hours resulted in a significant increase in diffusion, as shown in figure 18(b-1). After bonding, diffusion affected the IN-100 to a depth of 0.075 millimeter. After 200 hours the affected depth in the IN-100 increased by 7 percent; after 400 hours it increased by 28 percent. On the cladding side, the first 200 hours of oxidation exposure resulted in a significant increase (about 200 percent) in the diffusion-affected zone for all three elements. The second 200 hours of exposure, however, produced little further diffusion zone growth (about 10 percent). However, the cycle frequency effect on diffusion of Co, Ni, and Cr (fig. 18(b-2)) shows that no significant difference existed between 400 1-hour cycles and twenty 20-hour cycles at 1040° C. In both cases the depth of diffusion-affected zone in the IN-100 was 0.098 millimeter. As

would be expected, temperature exerted a larger influence on interdiffusion. Figure 18(b-3) shows that after ten 20-hour cycles, the Co, Ni, and Cr diffusion-affected zones in the cladding and in the substrate were 34 and 23 percent greater at 1090° C than at 1040° C.

Fe-Cr-Al-Y Clad IN-100 System

After 200 hours (20-hour cycles), the raster micrographs of figure 19(a) show the oxide scales on the Fe-Cr-Al-Y clad IN-100 specimens were rich in Al, Cr, and Fe; while Ni, Co, and Mo had diffused into the cladding, and Cr and Fe had diffused into the IN-100. A similar exposure at 1090° C resulted in mainly Al in the scale; a continuation of the Ni, Co, and Mo diffusion into the cladding; and a continuation of Cr and Fe diffusion into the substrate. Here, however, localized Ti-rich areas were seen to be present in the cladding and also in the oxide scale. Figure 19(b) contains line scan data presented in bar graph form, as in figure 18. The Al line scan data are not included since this element was near the limits of detection and small variations were hard to resolve. Even during bonding, Ni and Co diffused into the Fe-Cr-Al-Y clad on IN-100. After the 1040° C exposure, diffusion produced concentration gradients in Ni, Co, Fe, and Cr all across the cladding and relatively deep into the IN-100. Ni was detected in the oxide scale and its presence was felt to be detrimental to oxidation resistance. As compared to 1040° C oxidation, exposure for an equivalent time of 200 hours at 1090° C resulted in a substantial (about 84 percent) increase in the thickness of the diffusion-affected zone in the IN-100.

Ni-Cr-Si Clad IN-100 System

The raster micrographs of figure 20(a) indicate that the oxide scales on the Ni-Cr-Si clad IN-100 specimens contained only Cr, Si, Al, and Ti after 1040° C exposure and Ni, Cr, Al, Si, and Ti after 160 hours at 1090° C. At both temperatures the Si was probably present as amorphous SiO_2 and so was not detected by XRD. The raster micrographs showed (fig. 20(a)) that after 200 hours at 1040° C, Al, Ti, Co, and Mo had diffused into the cladding. The Al appeared to be present in intergranular oxides. With time at 1090° C, Co, Al, and Ti enter the cladding and the latter two concentrate in the scale and in the cladding - IN-100 interface. These data indicate that Al and Mo diffuse faster than Ti and Co at both temperatures. The line scan data in figure 20(b) show that the 0.127-millimeter cladding was completely affected by interdiffusion after oxidation at both temperatures. The diffusion gradients of Ni, Cr, and Co extended into the IN-100 to a depth of 0.100 and 0.120 millimeter after oxidation at

1040° and 1090° C, respectively. This is an increase of about five- and sixfold, respectively, over the as-bonded condition.

REFERENCES

1. Jackson, C. M.; and Hall, A. M.: Surface Treatments for Nickel and Nickel-Base Alloys. NASA TM X-53448, 1966.

2. Gedwill, Michael A.: An Evaluation of Three Oxidation-Resistant Alloy Claddings for IN 100 and WI 52 Superalloys. NASA TN D-5483, 1969.

3. Wood, Graham C.: High-Temperature Oxidation of Alloys. Oxidation of Metals, vol. 2, no. 1, Spring 1970, pp. 11-57.

4. Grisaffe, Salvatore J.; and Lowell, Carl E.: Examination of Oxide Scales on Heat Resisting Alloys. NASA TN D-5019, 1969.

TABLE I. - CHEMICAL ANALYSIS OF IN-100 SUBSTRATES AND CLADDING ALLOYS

Element	Content, wt. %			
	IN-100	Ni-20Cr-4Al-1.2Si	Fe-25Cr-4Al-1Y	Ni-30Cr-1.4Si
Ni	61.14	Balance	0.15	Balance
Co	15.37	0.03	.007	0.001
Fe	.20	.7	Balance	.15
Cr	9.50	19.54	24.82	29.63
Al	5.33	3.51	4.12	.3
Si	.08	1.22	.18	1.43
Ti	4.26	-------	-------	-------
Mo	3.17	-------	-------	-------
W	[a]<.05	[a]<.05	[a]<.05	[a]<.05
Cb	.10	-------	-------	-------
Mn	.003	.4	-------	.01
Y	------	-------	.58	-------
C	.166	.076	.0058	.028

[a]Not detected, less than the limits of defection.

TABLE II. - METALLOGRAPHIC MEASUREMENTS OF USEFUL REMAINING CLADDING ON CLAD CLADDING-ALLOY SPECIMENS AFTER OXIDATION AT 1040° AND 1090° C

System	Initial cladding thickness, mm	Oxidation			Average thickness of useful cladding after oxidation test (±0.005 mm), [a] mm	Remaining useful cladding thickness, percent
		Total number of cycles	Cycle time, hr	Total time, hr		
1040° C Oxidation						
Ni-20Cr-4Al-1.2Si clad Ni-20Cr-4Al-1.2Si	0.127±0.013	10	20	200	0.112	88
		20	20	400	.114	90
Fe-25Cr-4Al-1Y clad Fe-25Cr-4Al-1Y	0.254±0.025	10	20	200	0.235	93
Ni-30Cr-1.4Si clad Ni-30Cr-1.4Si	0.127±0.013	10	20	200	0.127	100
1090° C Oxidation						
Ni-20Cr-4Al-1.2Si clad Ni-20Cr-4Al-1.2Si	0.127±0.013	10	20	200	0.107	84
Fe-25Cr-4Al-1Y clad Fe-25Cr-4Al-1Y	0.254±0.025	10	20	200	0.233	92
		20	20	400	.224	88
Ni-30Cr-1.4Si clad Ni-30Cr-1.4Si	0.127±0.013	10	20	200	0.112	88
		20	20	400	.114	90

[a] Average of two measurements. Includes internal oxidation and voids, but not gross penetration of surface oxides. (See fig. 1.)

TABLE III. - METALLOGRAPHIC MEASUREMENTS OF USEFUL REMAINING CLADDING ON CLAD IN-100 SPECIMENS AFTER OXIDATION AT 1040° AND 1090° C

System	Initial cladding thickness, mm	Oxidation			Average thickness of useful cladding after oxidation test (±0.005 mm),[a] mm	Remaining useful cladding thickness, percent
		Total number of cycles	Cycle time, hr	Total time, hr		
1040° C Oxidation						
Ni-20Cr-4Al-1.2Si clad IN-100	0.051±0.010	5	20	100	0.041	80
		10	20	200	.041	80
		20	20	400	.041	80
		400	1	400	.038	75
	0.127±0.013	5	20	100	0.117	92
		10	20	200	.119	94
		20	20	400	.114	90
		400	1	400	.109	86
	0.254±0.013	400	1	400	0.220	87
Fe-25Cr-4Al-1Y clad IN-100	0.127±0.020	10	20	200	0.081	64
		20	20	400	.076	60
		400	1	400	.094	74
	0.254±0.025	10	20	200	0.234	92
Ni-30Cr-1.4Si clad IN-100	0.051±0.008	10	20	200	0.003	6
	0.127±0.013	10	20	200	0.069	54
		20	20	400	.041	32
	0.254±0.015	10	20	200	0.249	98
1090° Oxidation						
Ni-20Cr-4Al-1.2Si clad IN-100	0.051±0.010	10	20	200	0.033	65
	0.127±0.013	2	20	40	0.122	96
		10	20	200	.109	86
	0.254±0.013	10	20	200	0.228	90
Fe-25Cr-4Al-1Y clad IN-100	0.127±0.020	10	20	200	0.076	60
	0.254±0.025	10	20	200	0.224	88
		20	20	400	.200	79
Ni-30Cr-1.4Si clad IN-100	0.127±0.013	3	20	60	0.086	68
		8	20	160	.058	46
	0.254±0.015	10	20	200	0.213	84

[a]Average of two or three measurements. Includes internal oxidation and voids, but not gross penetration of surface oxides. (See fig. 1.)

TABLE IV. - X-RAY DIFFRACTION AND X-RAY FLUORESCENCE ANALYSES OF RETAINED SCALES AND SPALLS FROM CLAD IN-100 SPECIMENS AFTER CYCLIC OXIDATION

System	Original cladding thickness, mm	Oxidation			X-ray diffraction analysis					X-ray fluorescence analysis (elements showing change in intensity at specimen surface)[c]	
		Total number of cycles	Cycle time, hr	Total time, hr	Performed on -	Major constituents[a]	Spinel composition[b]	Minor constituents	Trace constituents	Increase	Decrease
1040° C Oxidation											
Ni-20Cr-4Al-1.2Si clad IN-100	0.051	5	20	100	Scraping	Spinel (a_o = 8.33±0.02 Å) + NiO	$NiCr_2O_4$	----------	Cr_2O_3 + αAl_2O_3	Ti, Mo, Co	Al
		10	20	200	↓	Spinel (a_o = 8.30±0.02 Å) + NiO	$NiCr_2O_4$	----------	Cr_2O_3	Si, Ti, Mo, Co	Al
		20	20	400		Spinel (a_o = 8.30±0.02 Å) + NiO	$NiCr_2O_4$	----------	----------	Si, Ti, Mo, Co	Al
		400	1	400		Spinel (a_o = 8.32±0.02 Å) + NiO	$(Ni, Co)Cr_2O_4$	----------	αAl_2O_3	Al, Si, Ti, Mo, Co	------
					Spall	Spinel (a_o = 8.28±0.02 Å) + NiO	(d)	----------	Cr_2O_3		
	0.127	5	20	100	In-situ scale	Spinel (a_o = 8.37±0.02 Å) + NiO	$NiCr_2O_4$	Cr_2O_3	αAl_2O_3	Si, Mo	Al
		10	20	200	Scraping	Spinel (a_o = 8.32±0.02 Å) + NiO[e]	$NiCr_2O_4$	----------	Cr_2O_3	Si, Mo	------
		20	20	400	Scraping	Spinel (a_o = 8.30±0.02 Å) + NiO	$NiCr_2O_4$	----------	Cr_2O_3	Mo, Co	Al
		400	1	400	In-situ scale	NiO	$NiAl_2O_4$	Spinel (a_o = 8.15±0.02 Å)	αAl_2O_3	Al, Si, Ti, Co	------
					Spall	Spinel (a_o = 8.30±0.02 Å) + NiO	(d)	Cr_2O_3	αAl_2O_3		
	0.254	400	1	400	In-situ scale	Spinel (a_o = 8.33±0.02 Å) + NiO	$NiCr_2O_4$	Cr_2O_3	----------	Al, Si	------
					Spall	Spinel (a_o = 8.32±0.02 Å) + NiO	(d)	----------	Cr_2O_3		
Fe-25Cr-4Al-1Y clad IN-100	0.127	10	20	200	Scraping	$(Cr, Fe)_2O_3$		----------	Spinel (a_o = 8.25±0.02 Å)[f] + αAl_2O_3	Ni, Co, Ti, Mo	Al
		20	20	400	Scraping	αAl_2O_3 + $(Cr, Fe)_2O_3$		----------	----------	Ni, Co, Ti, Mo	Al, Fe
		400	1	400	In-situ scale	αAl_2O_3 + $(Cr, Fe)_2O_3$		----------	Spinel (a_o = 8.25±0.02 Å)	----------	------
					Spall	$(Cr, Fe)_2O_3$ + spinel (a_o = 8.32±0.02 Å)	(d)	----------	αAl_2C_3		
	0.254	10	20	200	Scraping	αAl_2O_3		----------	----------	Ni, Co, Ti, Mo	------
Ni-30Cr-1.4Si clad IN-100	0.051	10	20	200	Scraping	Spinel (a_o = 8.28±0.02 Å) + NiO	$(Ni, Co)Cr_2O_4$	----------	Cr_2O_3 + $CoCrO_4$ + spinel (a_o = 8.05±0.02 Å)	Si, Co, Ti, Mo	Mn
	0.127	10	20	200	Scraping	Cr_2O_3		----------	----------	Ti, Mo	Al
		20	20	400	Scraping	Spinel (a_o = 8.33±0.02 Å) + Cr_2O_3	$NiCr_2O_4$	----------	----------	Ti, Mo, Co	Al
	0.254	10	20	200	In-situ scale	Cr_2O_3		----------	----------	Mo	Fe
1090° C Oxidation											
Ni-20Cr-4Al-1.2Si clad IN-100	0.051	10	20	200	Scraping	Spinel (a_o = 8.28±0.02 Å) + NiO	$(Ni, Co)Cr_2O_4$	----------	Spinel (a_o = 8.07±0.02 Å)	Al, Si, Co, Ti, Mo	------
	0.127	2	20	40	Scraping	Spinel (a_o = 8.30±0.02 Å) + NiO	$NiCr_2O_4$	----------	Cr_2O_3	Al, Si, Mo	------
		10	20	200	Scraping	Spinel (a_o = 8.20±0.02 Å) + NiO	$NiCr_2O_4$	----------	Spinel (a_o = 8.05±0.02 Å)	Al, Si, Co, Ti, Mo	------
	0.254	10	20	200	Scraping	Spinel (a_o = 8.30±0.02 Å) + NiO	$NiCr_2O_4$	----------	Spinel (a_o = 8.09±0.02 Å) + αAl_2O_3	Al, Si, Fe	------
Fe-25Cr-4Al-1Y clad IN-100	0.127	10	20	200	Scraping	αAl_2O_3[f] + $(Cr, Fe)_2O_3$		----------	----------	Co, Ti, Mo, Ni	Al
	.254	10	20	200	Scraping	αAl_2O_3		$(Cr, Fe)_2O_3$	----------	Co, Ti, Mo, Ni	Al
Ni-30Cr-1.4Si clad IN-100	0.127	3	20	60	Scraping	Cr_2O_3		----------	----------	Si, Ti	Al
		8	20	160	Scraping	Cr_2O_3 + spinel (a_o = 8.30±0.02 Å)	$(Ni, Co)(Cr, Al)_2O_4$	----------	----------	Al, Ni, Co, Ti, Mo	Mn
	0.254	10	20	200	Scraping	Cr_2O_3		----------	----------	----------	Al, Fe

[a] Lattice parameter, a_o; $NiCr_2O_4$, 8.32 Å; $NiAl_2O_4$, 8.10 Å.

[b] As a major or minor constituent based on X-ray fluorescence analysis.

[c] Based on intensity change compared to data obtained on cladding-alloy specimens oxidized at the same temperature for ten 20-hour cycles (data in ref. 2). For very low sensitive elements (W, Al, and Si) an increase of ≥50 percent and a decrease of ≤33 percent. For all other elements an increase of ≥200 percent and a decrease of ≤66 percent.

[d] Not determined.

[e] Not reported in ref. 2.

[f] Erroneously reported as a minor constituent in ref. 2.

TABLE V. - SUMMARY OF ELECTRON MICROPROBE ANALYSIS ON CLAD CLADDING-ALLOY AND CLAD IN-100[a] SPECIMENS AFTER CYCLIC OXIDATION

System	Oxidation			X-ray raster micrographs		Line (concentration) scans (elements in oxide scale)	
	Total number of cycles	Cycle time, hr	Total time, hr	Elements analyzed	Elements definitely present in oxide scales	Yes	No[b]
1040° C Oxidation							
Ni-20Cr-4Al-1.2Si clad Ni-20Cr-4Al-1.2Si	10	20	200	Ni, Cr, Al, Si, Mn, Fe	Ni, Cr, Al, Si, Mn, Fe	(c)	(c)
Ni-20Cr-4Al-1.2Si clad IN-100	10	20	200	Ni, Cr, Al, Si, Mn, Co, Ti, Fe, Mo	Ni, Cr, Al, Si, Mn	Ni, Cr	Co
	20	20	400	Ni, Cr, Al, Si, Mn, Co, Ti, Fe, Mo	Ni, Cr, Al, Si, Mn	Ni, Cr	Co*
	400	1	400	Ni, Cr, Al, Si, Mn, Co, Ti, Fe, Mo	Ni, Cr, Al, Si, Mn	Ni, Cr, Al	---
Fe-25Cr-4Al-1Y clad Fe-25Cr-4Al-1Y	10	20	200	Fe, Cr, Al, Si, Mn	Fe, Cr, Al	(c)	(c)
Fe-25Cr-4Al-1Y clad IN-100	10	20	200	Fe, Cr, Al, Ni, Co, Ti, Mo, C	Fe, Cr, Al	Fe, Cr, Ni	Co*
Ni-30Cr-1.4Si clad Ni-30Cr-1.4Si	10	20	200	Ni, Cr, Si, Mn	Cr, Si	(c)	(c)
Ni-30Cr-1.4Si clad IN-100	10	20	200	Ni, Cr, Si, Mn, Ti, Co, Al, Mo, C	Cr, Si, Al, Ti	Cr	Ni*, Co
1090° C Oxidation							
Ni-20Cr-4Al-1.2Si clad Ni-20Cr-4Al-1.2Si	10	20	200	Ni, Cr, Al, Si, Mn, Fe	Ni, Cr, Al, Mn, Fe	(c)	(c)
Ni-20Cr-4Al-1.2Si clad IN-100	2	20	40	Ni, Cr, Al, Si, Mn, Co, Ti, Fe, Mo	Ni, Cr, Al, Si, Mn, Fe, Mo	(c)	(c)
	10	20	200	Ni, Cr, Al, Si, Mn, Co, Ti, Fe	Ni, Cr, Al, Si, Mn, Fe	Ni, Cr	Co*
Fe-25Cr-4Al-1Y clad Fe-25Cr-4Al-1Y	10	20	200	Fe, Cr, Al, Ni, Co	Al	(c)	(c)
	20	20	400	Fe, Cr, Al	Al	(c)	(c)
Fe-25Cr-4Al-1Y clad IN-100	10	20	200	Fe, Cr, Al, Ni, Co, Ti, Mo	Fe, Cr, Al, Ti	Fe, Cr, Al, Ni	Co*
Ni-30Cr-1.4Si clad Ni-30Cr-1.4Si	10	20	200	Ni, Cr, Si, Mn, Fe	Cr, Si	(c)	(c)
Ni-30Cr-1.4Si clad IN-100	3	20	60	Ni, Cr, Si, Mn, Ti, Co, Mo, Al	Cr, Si, Al	(c)	(c)
	8	20	160	Ni, Cr, Si, Ti, Co, Mo, Al	Ni, Cr, Si, Al, Ti	Ni, Cr	Co*

[a]Original cladding thickness, 0.127 mm.

[b]Element with an asterisk is present below, but apparently not within, the oxide scale.

[c]Not determined.

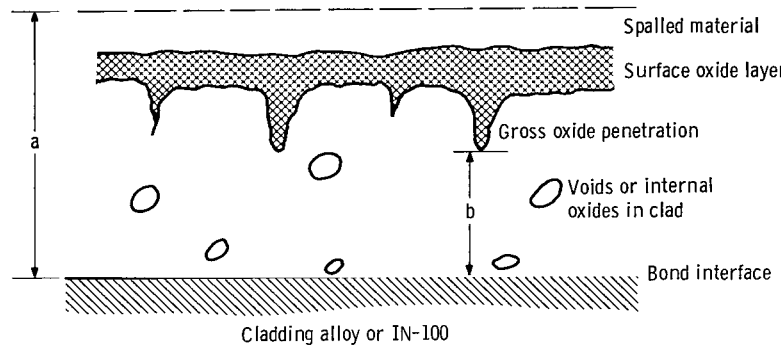

Figure 1. - Method of calculating surface recession using metallographic measurements of remaining useful cladding. Surface recession (plus gross oxide penetration) = a - b, where a is the original cladding thickness and b is the remaining useful cladding thickness (clad unaffected by gross oxidation and oxide penetration).

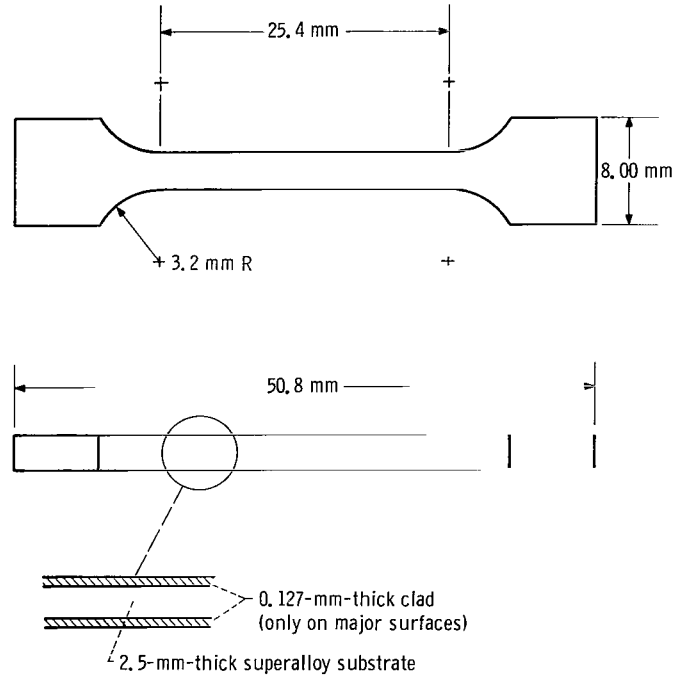

Figure 2. - Tensile specimen design.

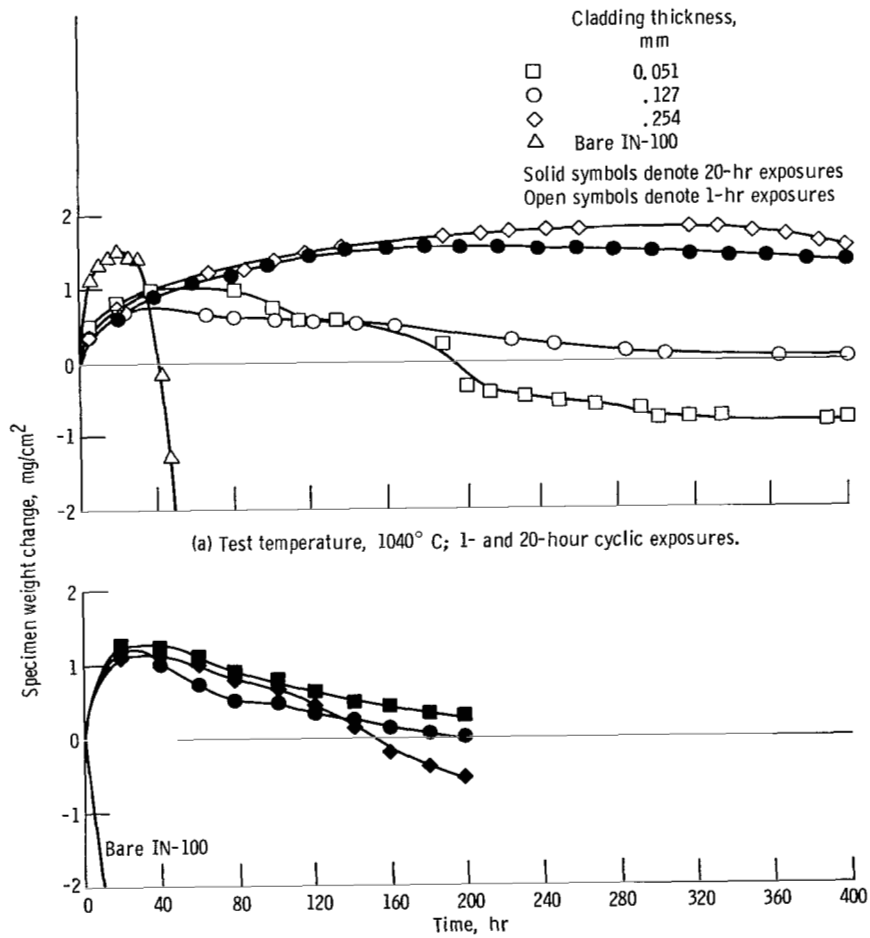

(a) Test temperature, 1040° C; 1- and 20-hour cyclic exposures.

(b) Test temperature, 1090° C; 20-hour cyclic exposures.

Figure 3. - Effect of cladding thickness on cyclic oxidation of Ni-20Cr-4Al-1.2Si clad IN-100 at 1040° and 1090° C.

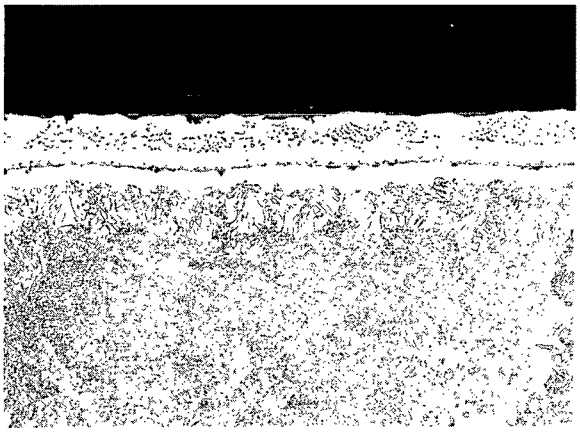

(a) Cladding thickness, 0.051 millimeter.

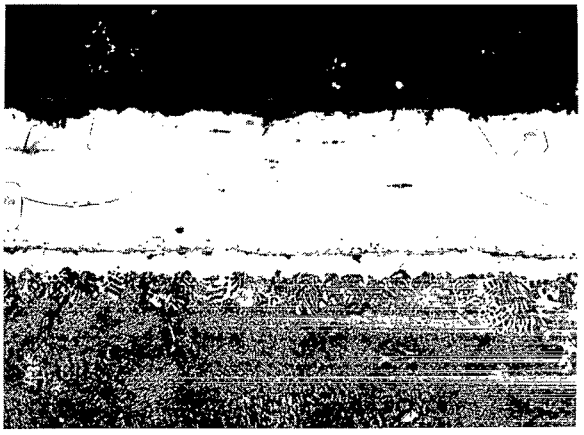

(b) Cladding thickness, 0.127 millimeter.

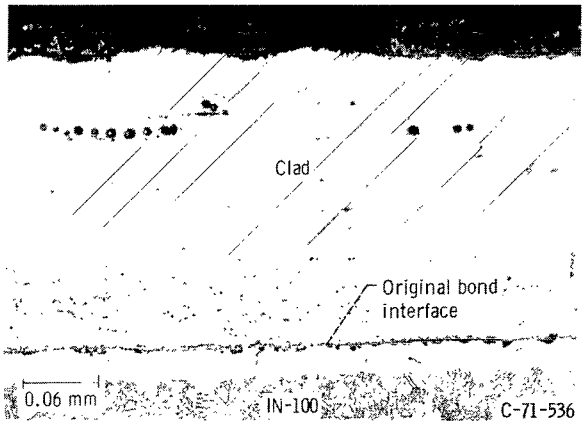

(c) Cladding thickness, 0.254 millimeter.

Figure 4. - Microstructures of Ni-20Cr-4Al-1.2Si clad IN-100 of three different cladding thicknesses after 1040° C oxidation for 400 1-hour exposures. X250.

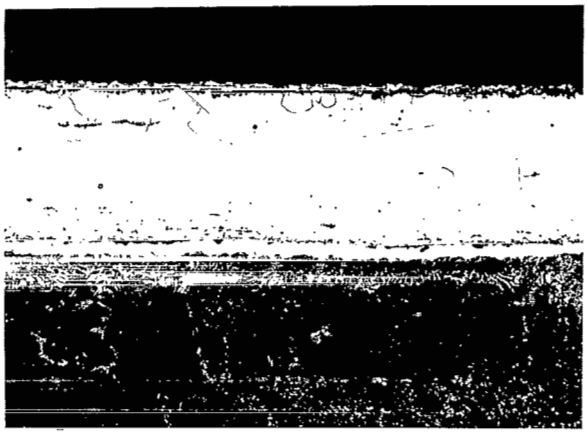

(a-1) After five cycles.

(a-2) After 10 cycles.

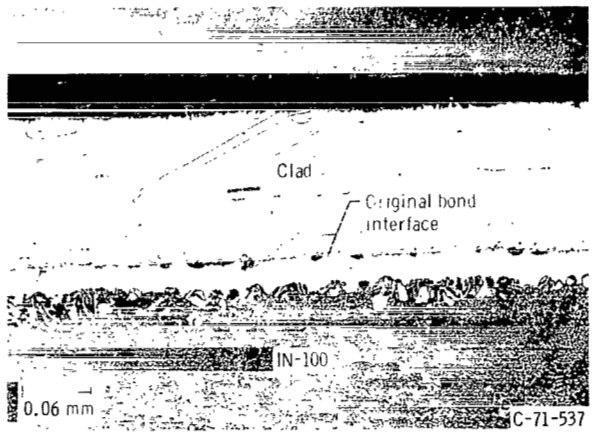

(a-3) After 20 cycles.

(a) Number of 20-hour exposures at 1040° C.

Figure 5. - Microstructures showing effect of cycling and temperature on oxidation behavior of Ni-20Cr-4Al-1.2Si clad IN-100 system. X250.

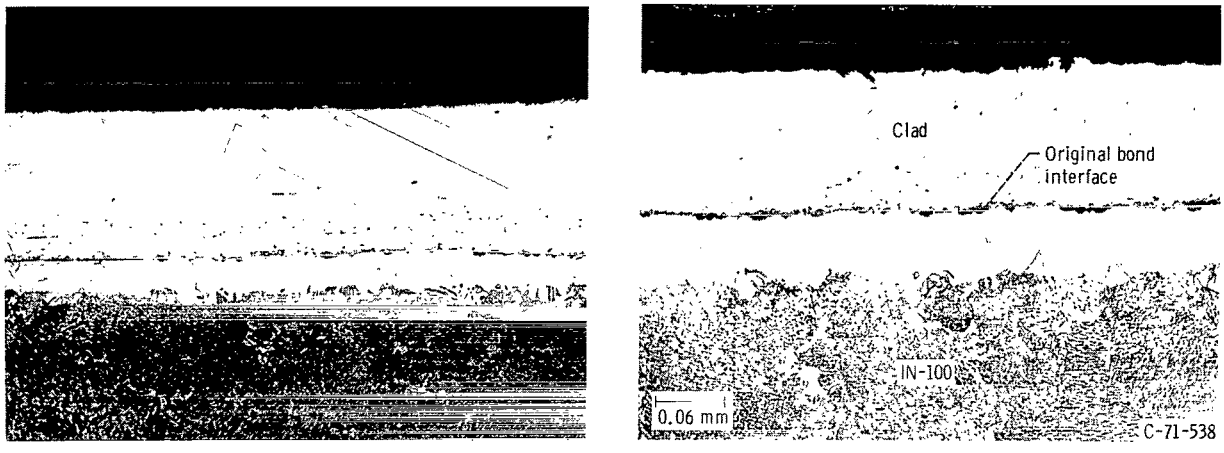

(b-1) After two cycles.

(b-2) After 10 cycles.

(b) Number of 20-hour exposures at 1090° C.

Figure 5. - Concluded.

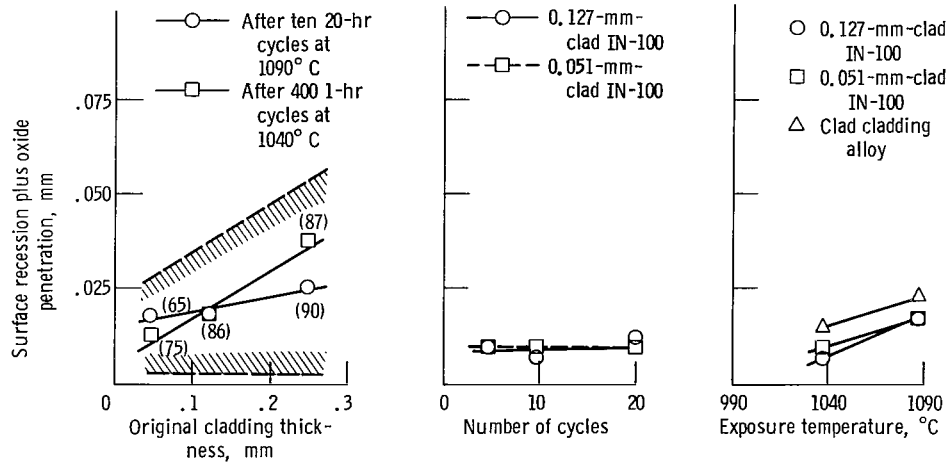

(a) Effect of original cladding thickness and cyclic frequency. Remaining useful cladding thicknesses in percentages are given in parentheses (from table III).

(b) Effect of total cycling; 1040° C oxidation; 20-hr cycles.

(c) Effect of exposure temperature after ten 20-hour cycles.

Figure 6. - Summary of total surface recession plus oxide penetration data for Ni-20Cr-4Al-1.2Si clad IN-100 system.

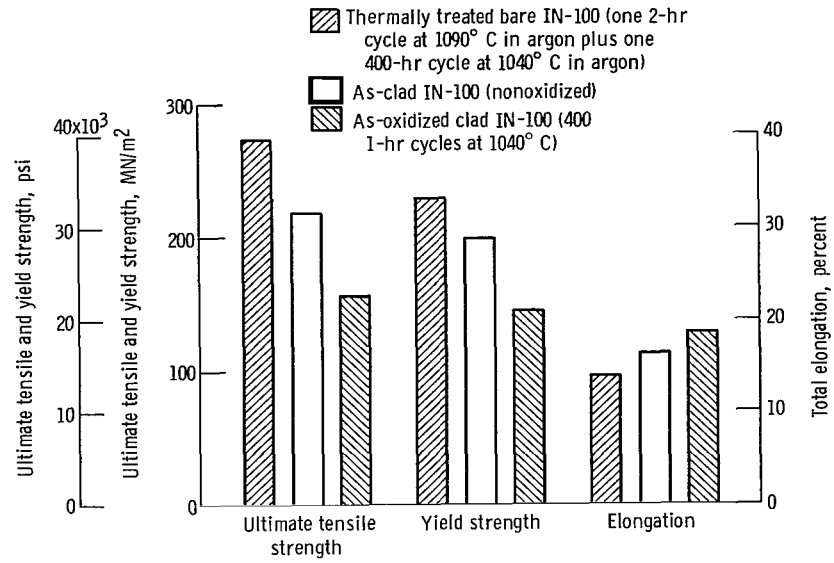

Figure 7. - Comparison of tensile properties of Ni-20Cr-4Al-1.2Si clad IN-100 at 1040° C before and after oxidation.

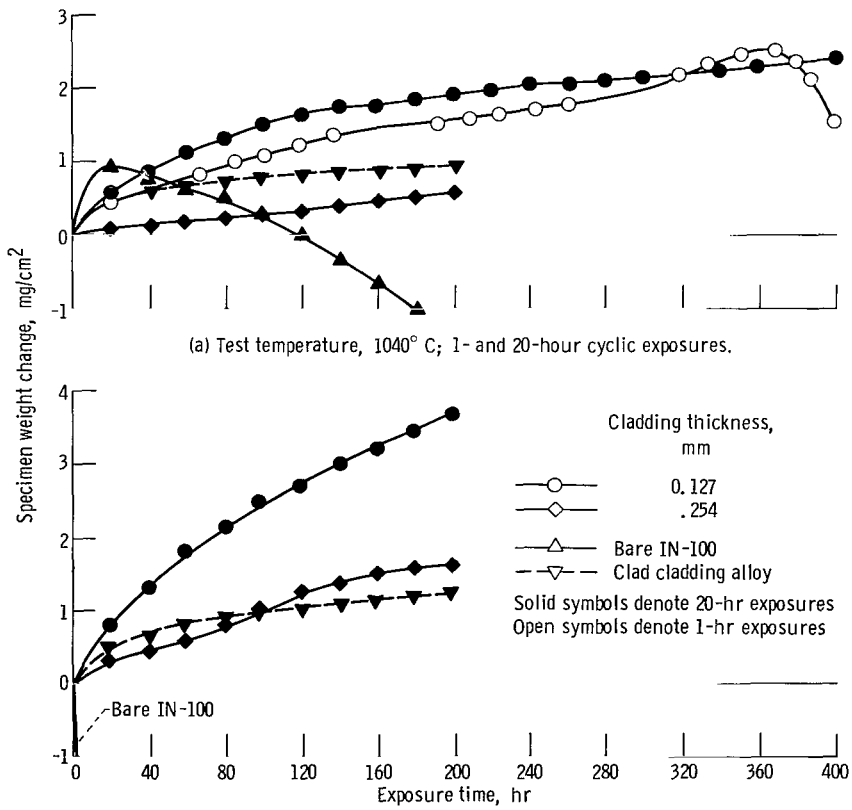

(a) Test temperature, 1040° C; 1- and 20-hour cyclic exposures.

(b) Test temperature, 1090° C; 20-hour cyclic exposures.

Figure 8. - Effect of cladding thickness, cycle frequency, and temperature on cyclic oxidation of Fe-25Cr-4Al-1Y clad IN-100 at 1040° and 1090° C.

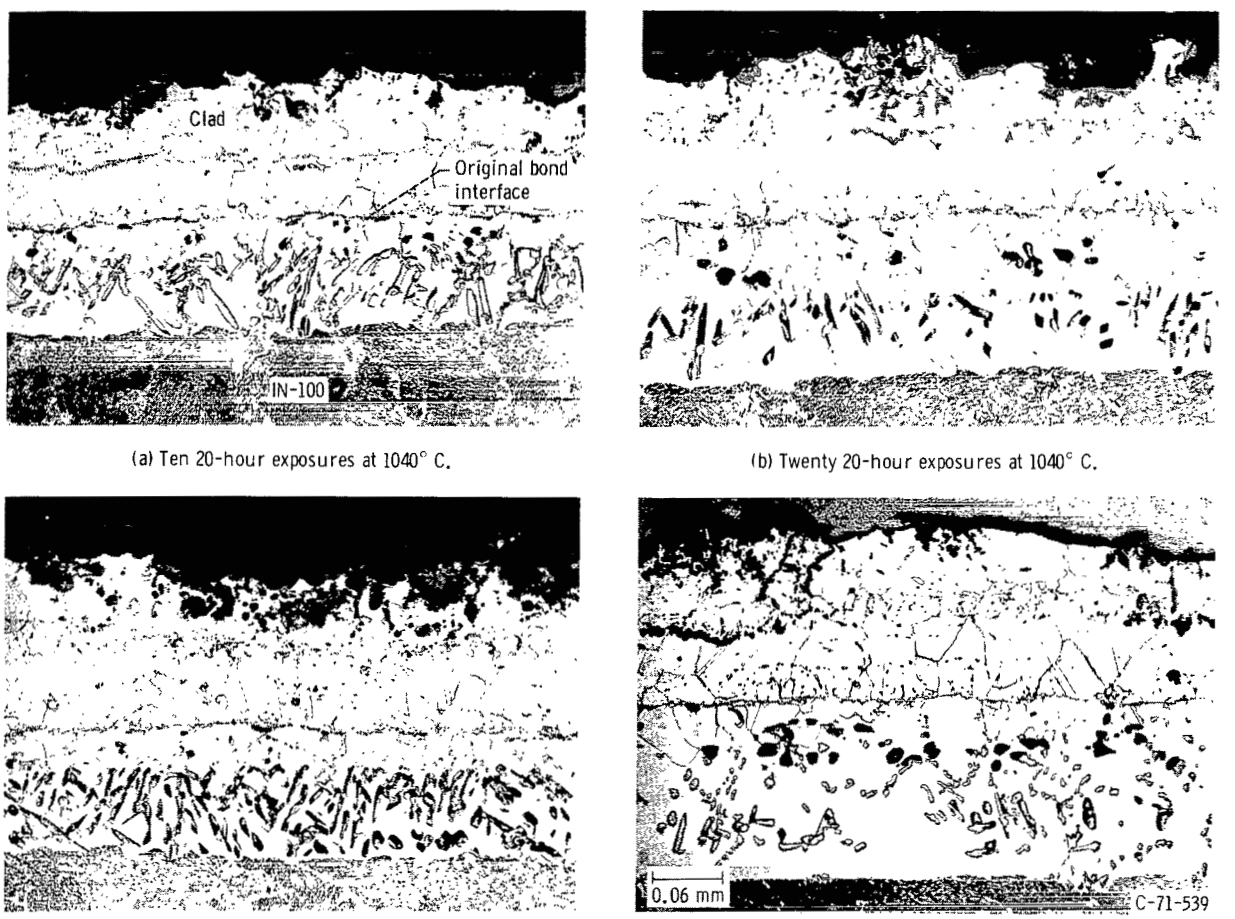

(a) Ten 20-hour exposures at 1040° C.

(b) Twenty 20-hour exposures at 1040° C.

(c) 400 1-hour exposures at 1040° C.

(d) Ten 20-hour exposures at 1090° C.

Figure 9. - Photomicrographs showing effects of cycling, cycle frequency, and temperature on microstructures of Fe-25Cr-4Al-1Y clad IN-100 after oxidation. Cladding thickness, 0.127 millimeter. X250.

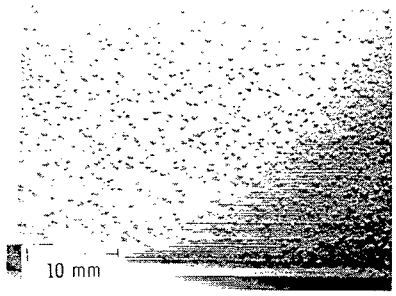

(a) Photograph (~X2) showing nodules formed on exterior surface (only above IN-100 substrate) of an oxidized specimen. Bright-field illumination.

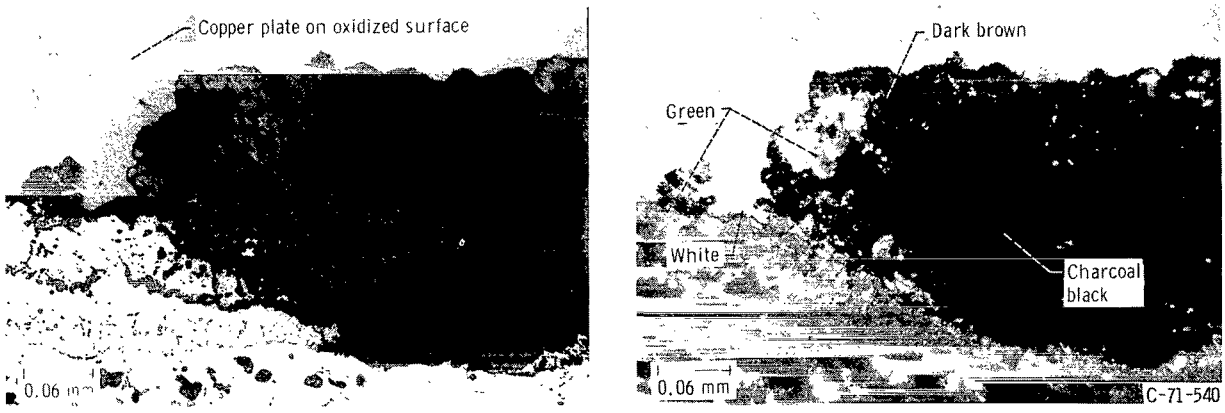

(b-1) Bright-field illumination.

(b-2) Polarized-light illumination.

(b) Cross sections of oxidized specimen showing one of the largest nodules in (a). X250.

Figure 10. - External and internal features of Fe-25Cr-4Al-1Y clad IN-100 oxidized for ten 20-hour exposures at 1090° C. Cladding thickness, 0.127 millimeter.

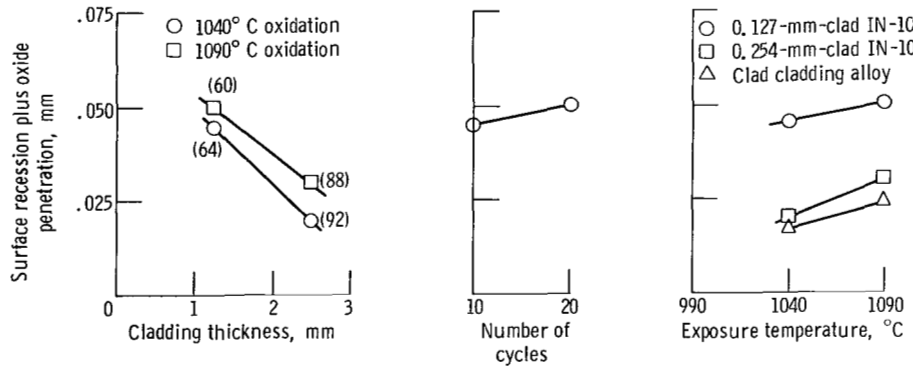

(a) Effect of original cladding thickness after ten 20-hour cycles. Remaining useful cladding thicknesses in percentages are given in parentheses (from table III).

(b) Effect of total cycling for a 0.127-millimeter clad thickness; 1040° C oxidation; 20-hour cycles.

(c) Effect of exposure temperature after ten 20-hour cycles.

Figure 11. - Summary of surface recession plus oxide penetration data for Fe-25Cr-4Al-1Y clad IN-100 system.

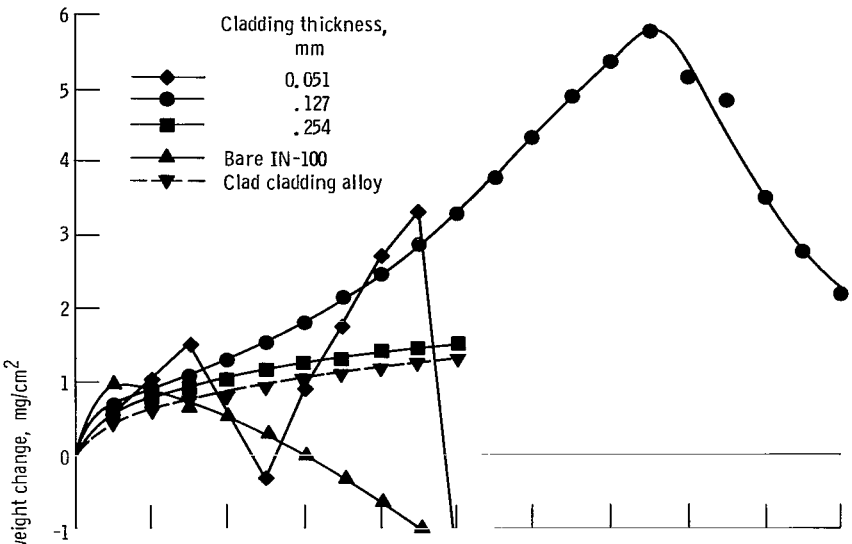

(a) Test temperature, 1040° C; 20-hour cyclic exposures.

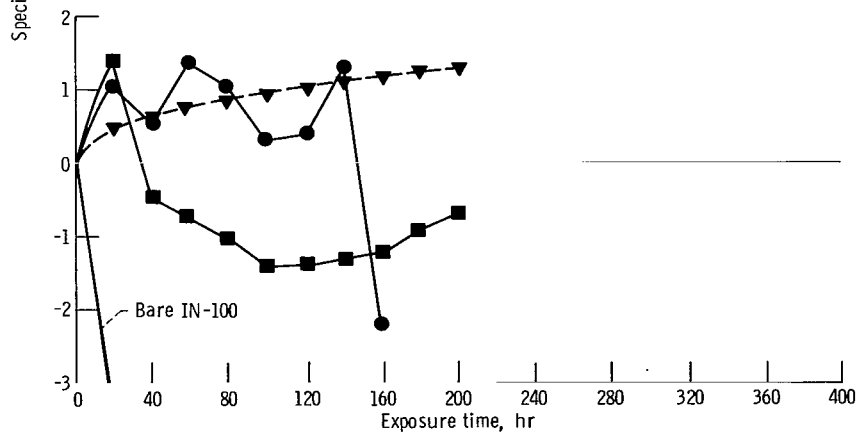

(b) Test temperature, 1090° C; 20-hour cyclic exposures.

Figure 12. - Effect of cladding thickness and temperature on cyclic oxidation of Ni-30Cr-1.4Si clad IN-100.

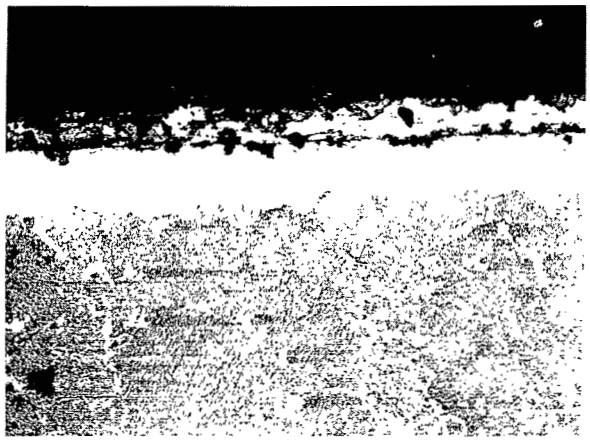

(a) 0.051-Millimeter-clad IN-100 after ten 20-hour exposures at 1040° C.

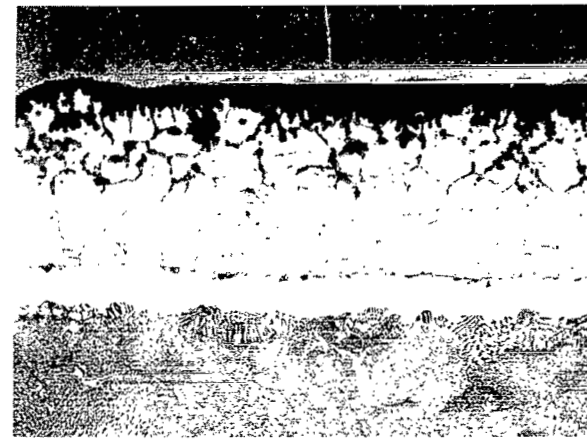

(b) 0.127-Millimeter-clad IN-100 after ten 20-hour exposures at 1040° C.

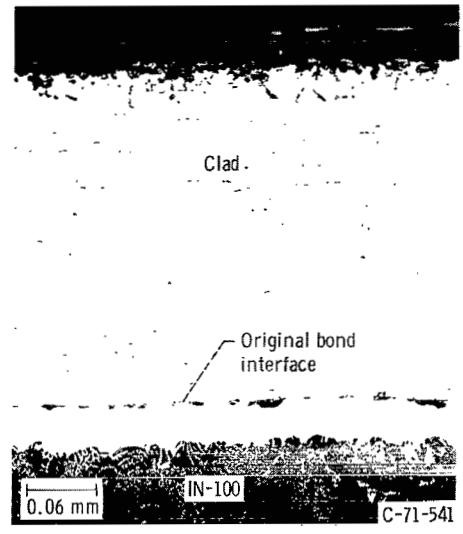

(c) 0.254-Millimeter-clad IN-100 after ten 20-hour exposures at 1040° C.

Figure 13. - Photomicrographs showing effects of cladding thickness, cycling, and temperature on microstructures of Ni-30Cr-1.4Si clad IN-100 after oxidation. X250.

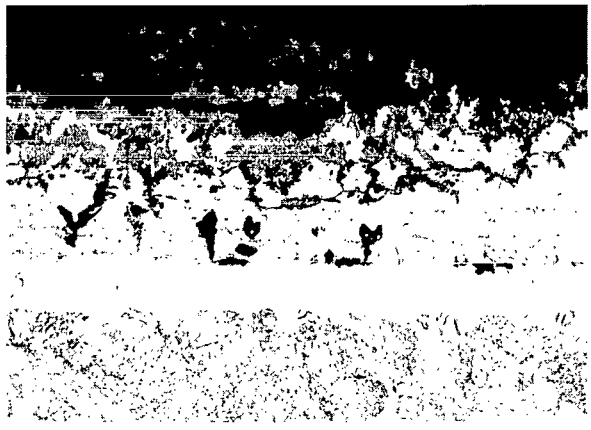

(d) 0.127-Millimeter-clad IN-100 after twenty 20-hour exposures at 1040° C.

(e) 0.127-Millimeter-clad IN-100 after eight 20-hour exposures at 1090° C.

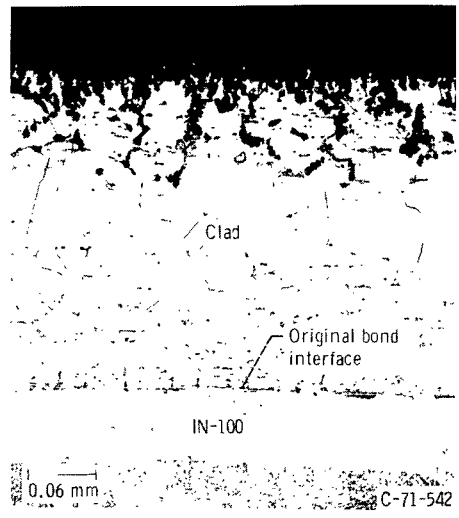

(f) 0.254-Millimeter-clad IN-100 after ten 20-hour exposures at 1090° C.

Figure 13. - Concluded.

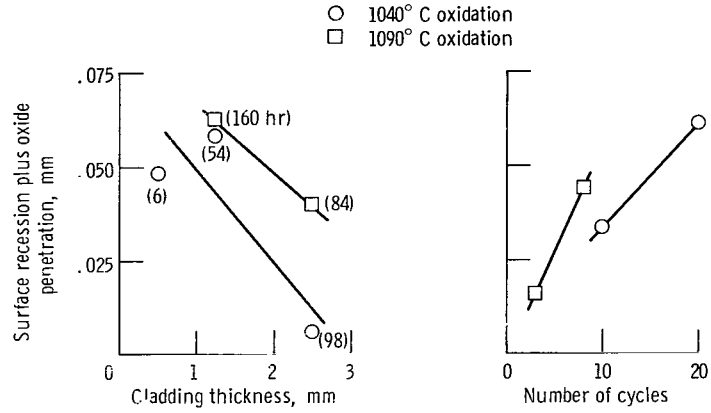

(a) Effect of cladding thickness and temperature, after ten 20-hour exposures (except where noted). Remaining useful cladding thicknesses in percentages are given in parentheses (from table III).

(b) Effect of cycling for a 0.127-millimeter clad thickness; 20-hour exposure cycles.

Figure 14. - Summary of total surface recession plus oxide penetration data for Ni-30Cr-1.4Si clad IN-100.

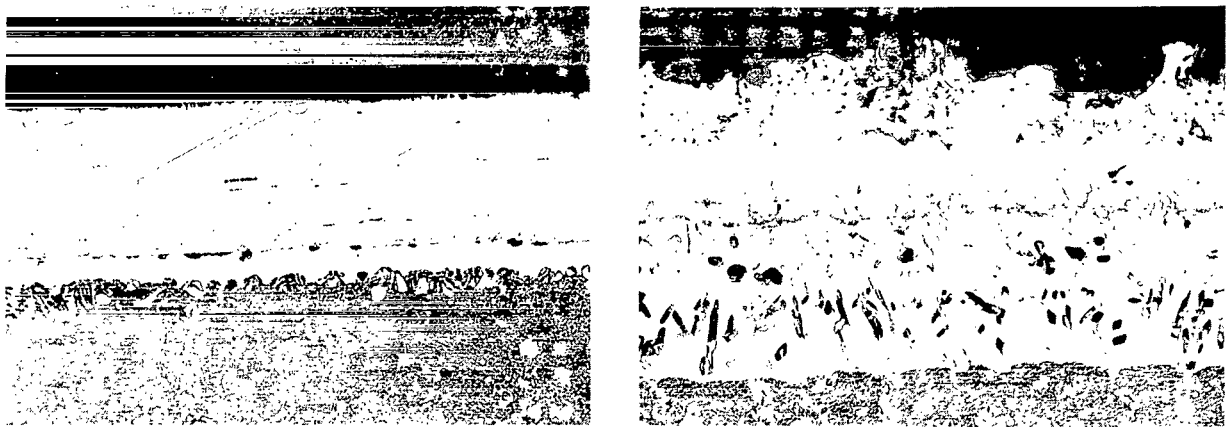

(a) Ni-20Cr-4Al-1.2Si clad IN-100.

(b) Fe-25Cr-4Al-1Y clad IN-100.

(c) Ni-30Cr-1.4Si clad IN-100.

Figure 15. - Comparison of microstructures of the three clad IN-100 systems after the 20-hour exposures in air at 1040° C. Cladding thickness, 0.127 millimeter. X250.

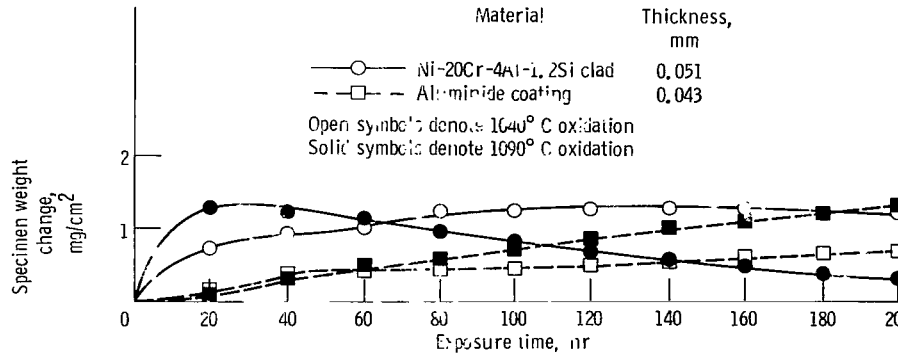

Figure 16. - Comparison of cyclic oxidation resistance of Ni-20Cr-4Al-1.2Si clad IN-100 and commercial aluminide-coated IN-100 at 1040° and 1090° C. Twenty-hour cyclic exposures.

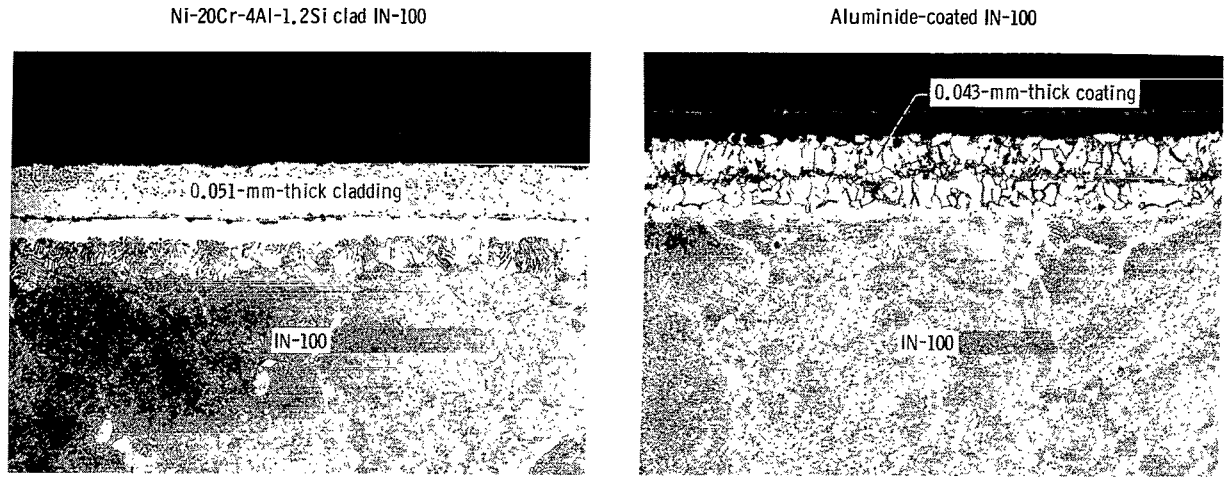

(a) After ten 20-hour exposures at 1040° C.

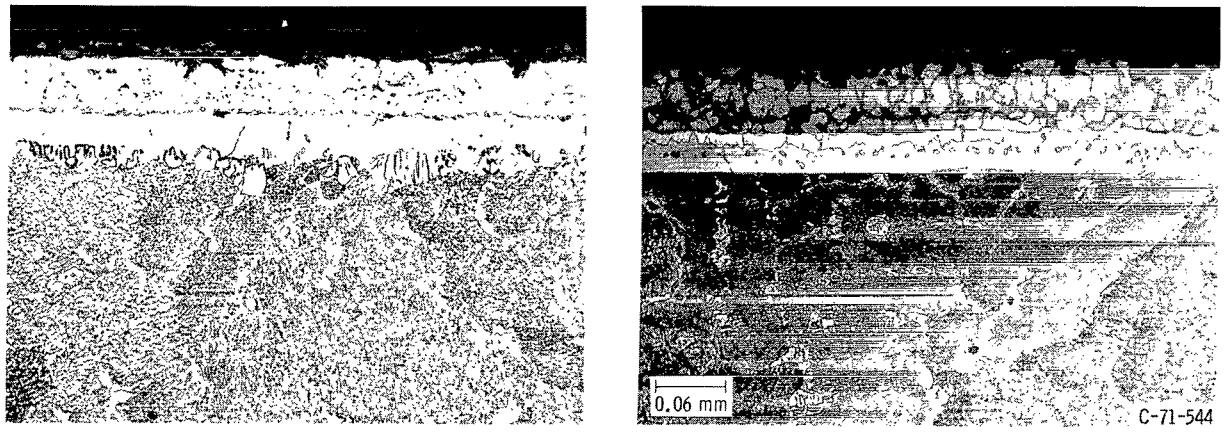

(b) After ten 20-hour exposures at 1090° C.

Figure 17. - Comparison of cyclic furnace oxidation on microstructures of Ni-20Cr-4Al-1.2Si clad IN-100 and a commercial aluminide-coated IN-100.

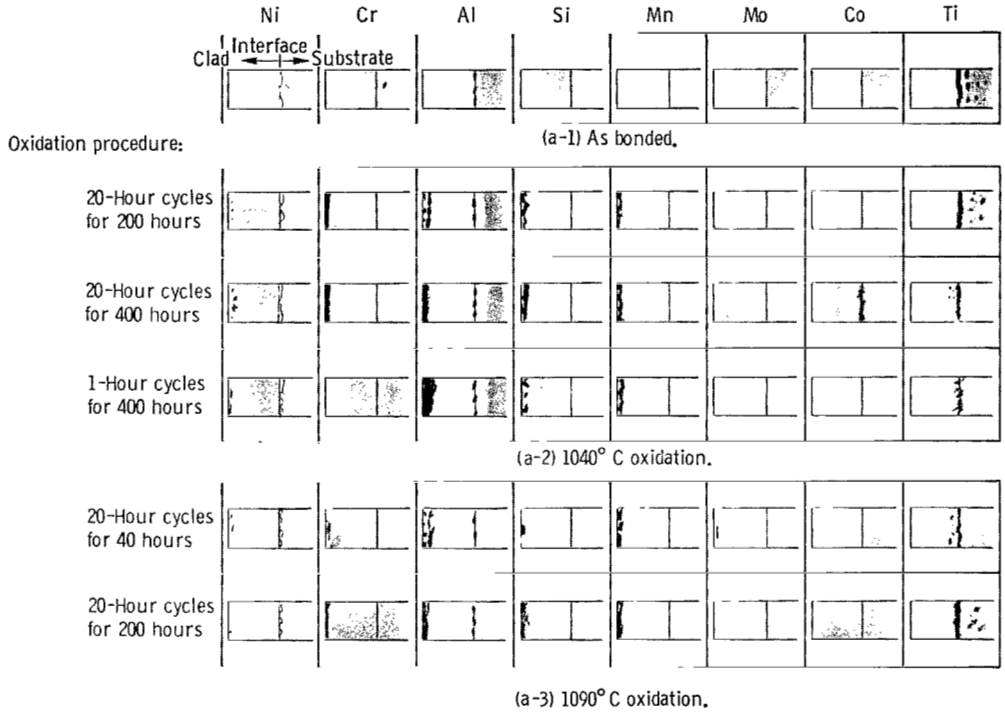

(a) Schematic of raster micrographs. (An increase in X-ray intensity is represented by a corresponding increase in darkness.)

Figure 18. - Schematic of electron microprobe raster micrographs and extent of interdiffusion of major elements of Ni-20Cr-4Al-1.2Si clad IN-100 after bonding and oxidation.

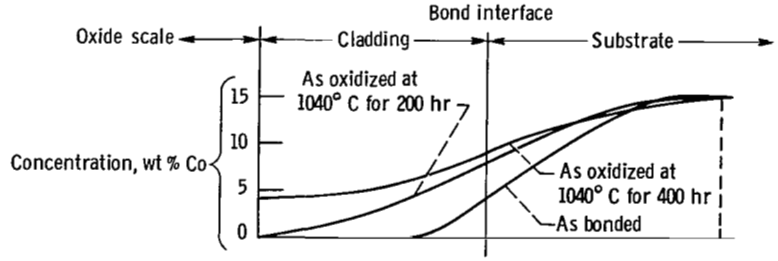

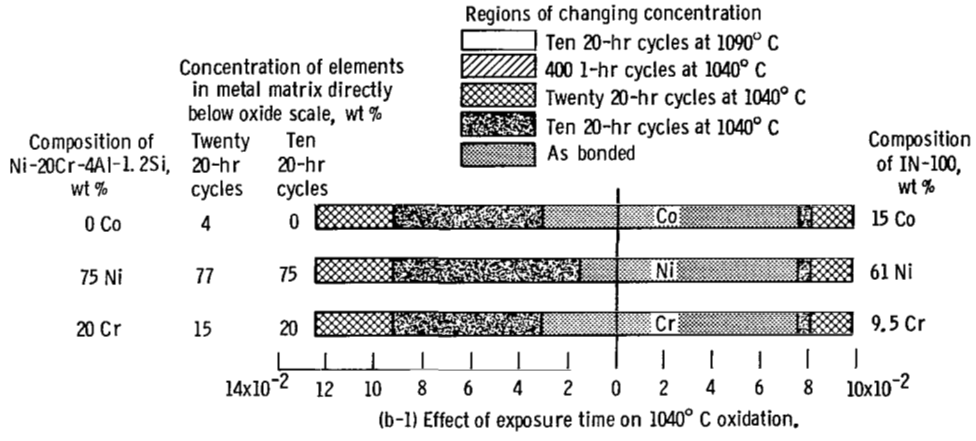

(b-1) Effect of exposure time on 1040° C oxidation.

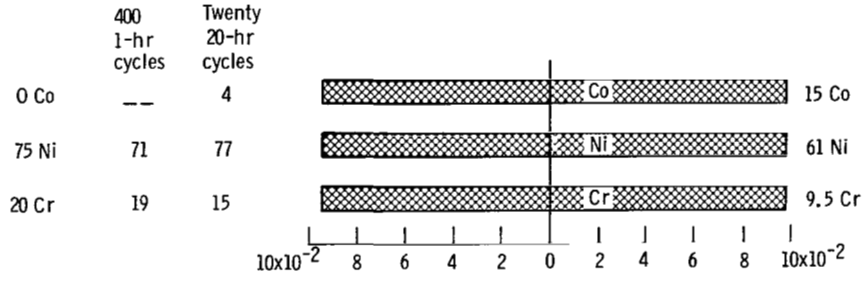

(b-2) Effect of cycle frequency at 1040° C oxidation. (Line scan for cobalt after 400 1-hr cycles was not made.)

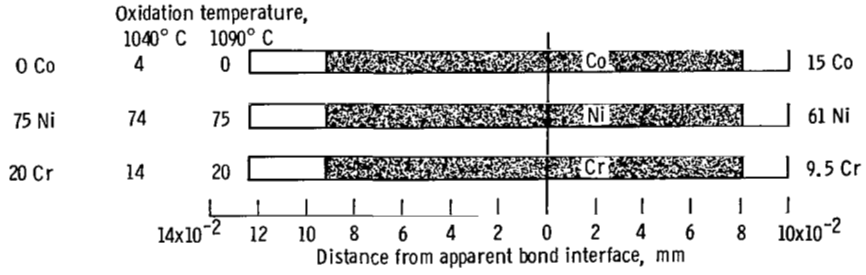

(b-3) Effect of maximum oxidation temperature. Maximum temperatures, 1040° and 1090° C; ten 20-hour cyclic exposures.

(b) Line scan data. (Concentrations in metal matrix are based on element concentrations in unaltered substrate, i.e., uncorrected X-ray intensity data normalized to analyzed chemical composition of IN-100.)

Figure 18. - Concluded.

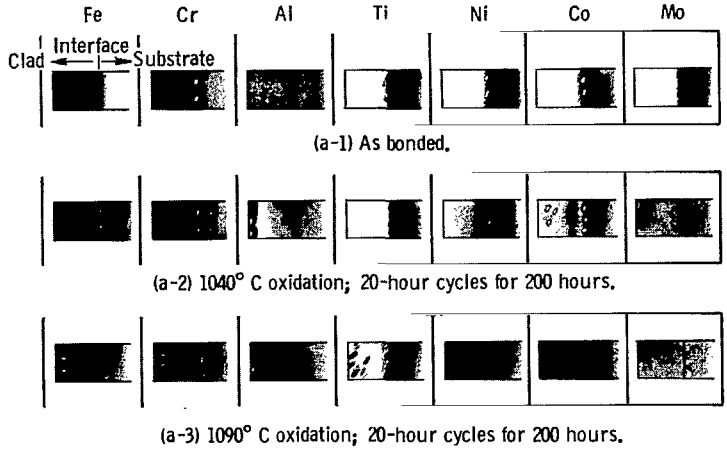

(a-1) As bonded.

(a-2) 1040° C oxidation; 20-hour cycles for 200 hours.

(a-3) 1090° C oxidation; 20-hour cycles for 200 hours.

(a) Schematic of raster micrographs. (An increase in X-ray intensity is represented by a corresponding increase in darkness.)

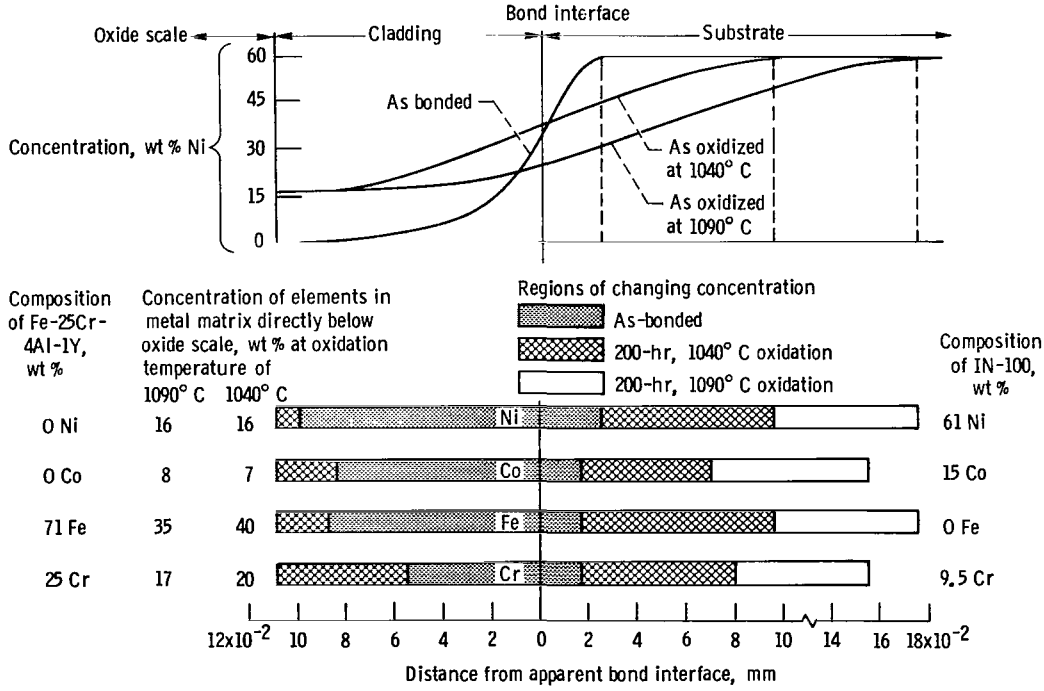

(b) Line scan data. (Except for using pure metal standard for iron, concentrations in metal matrix are based on element concentrations in unaltered substrate, i.e., uncorrected X-ray intensity data normalized to analyzed chemical composition of IN-100.)

Figure 19. - Schematic of electron microprobe raster micrographs and extent of interdiffusion of major elements in Fe-25Cr-4Al-1Y clad IN-100 before and after oxidation.

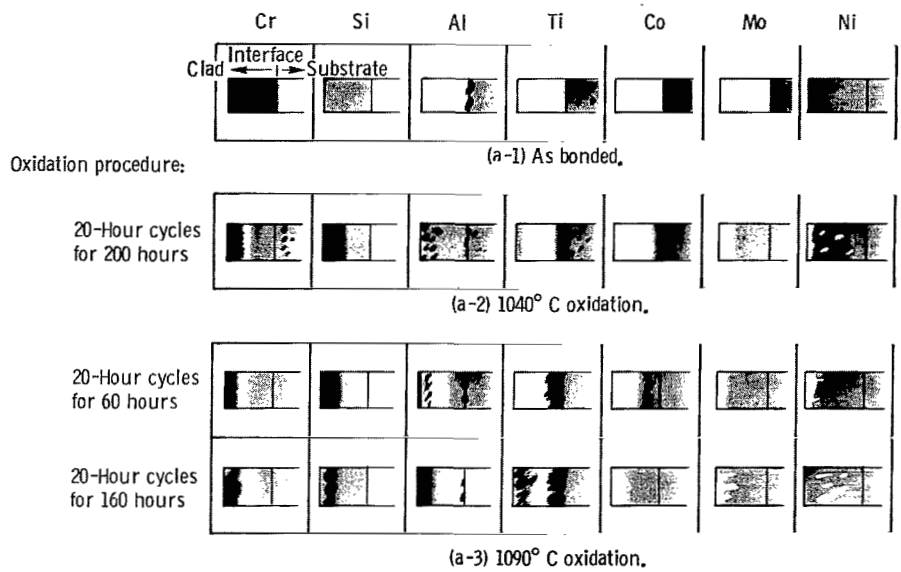

(a) Schematic of raster micrographs. (An increase in X-ray intensity is represented by a corresponding increase in darkness.)

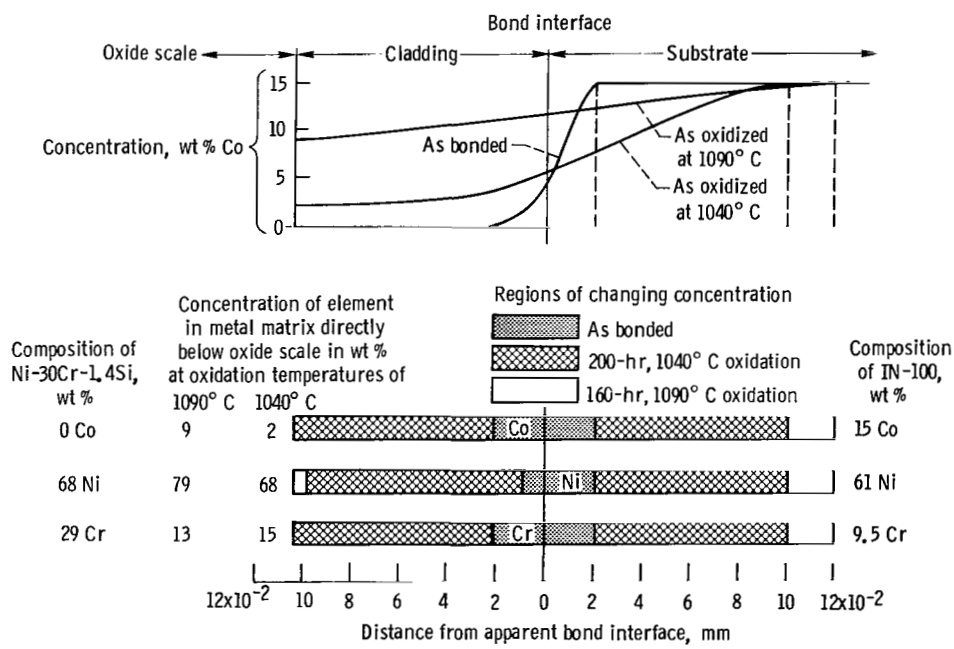

(b) Line scan data. (Concentrations in metal matrix are based on element concentrations in unaltered substrate; i.e., uncorrected X-ray intensity data normalized to analyzed chemical composition of IN-100.)

Figure 20. - Schematic of electron microprobe raster micrographs and extent of interdiffusion of major elements of Ni-30Cr-1.4Si clad IN-100 after bonding and oxidation.